

SPD 600-02

AD-A152 036

CUSHION PRESSURE INFLUENCES ON A HIGH LENGTH-TO-BEAM
RATIO SURFACE EFFECT SHIP IN IRREGULAR WAVES

DAVID W. TAYLOR NAVAL SHIP RESEARCH AND DEVELOPMENT CENTER

Bethesda, Md. 20084



CUSHION PRESSURE INFLUENCES ON A HIGH
LENGTH-TO-BEAM RATIO SURFACE EFFECT SHIP IN
IRREGULAR WAVES

by
Joseph J. Ricci
and
David D. Moran

APPROVED FOR PUBLIC RELEASE: DISTRIBUTION UNLIMITED

DTIC FILE COPY

SHIP PERFORMANCE DEPARTMENT

SELECTED
APR 9 1985
A

APRIL 1976

SPD 600-02

UNCLASSIFIED

SECURITY CLASSIFICATION OF THIS PAGE (When Data Entered)

REPORT DOCUMENTATION PAGE		READ INSTRUCTIONS BEFORE COMPLETING FORM	
1. REPORT NUMBER SPD 600-02	2. GOVT ACCESSION NO.	3. RECIPIENT'S CATALOG NUMBER	
4. TITLE (and Subtitle) Cushion Pressure Influences on a High Length-To-Beam Ratio Surface Effect Ship in Irregular Waves		5. TYPE OF REPORT & PERIOD COVERED	
		6. PERFORMING ORG. REPORT NUMBER	
7. AUTHOR(s) Joseph J. Ricci and David D. Moran		8. CONTRACT OR GRANT NUMBER(s)	
9. PERFORMING ORGANIZATION NAME AND ADDRESS Ship Performance Department High Performance Craft-Dynamics Branch Code 1572		10. PROGRAM ELEMENT, PROJECT, TASK AREA & WORK UNIT NUMBERS	
11. CONTROLLING OFFICE NAME AND ADDRESS		12. REPORT DATE April 1976	
		13. NUMBER OF PAGES 57	
14. MONITORING AGENCY NAME & ADDRESS (if different from Controlling Office)		15. SECURITY CLASS. (of this report) UNCLASSIFIED	
		15a. DECLASSIFICATION/DOWNGRADING SCHEDULE	
16. DISTRIBUTION STATEMENT (of this Report) Approved for Public Release: Distribution Unlimited			
17. DISTRIBUTION STATEMENT (of the abstract entered in Block 20, if different from Report)			
18. SUPPLEMENTARY NOTES			
19. KEY WORDS (Continue on reverse side if necessary and identify by block number) High Length to Beam Ratio; Cushion Pressure Distribution; Surface Effect Ship Wave Modification; Irregular Seakeeping <i>ACVC's in air supported vehicles</i>			
20. ABSTRACT (Continue on reverse side if necessary and identify by block number) Mathematical models developed for air-cushion-supported vehicles generally approximate the air pressure as being uniformly distributed within the cushion of the vehicle and assume that the pressure has no effect on the encountered wave field. The validity of these approximations is examined experimentally by measuring the spatial and temporal distribution of the air pressure in and wave elevation under the cushion of a high length-to-beam ratio surface effect ship model which is free to heave and pitch in irregular head waves. It is observed that the pressure is distributed nonuniformly			

DD FORM 1 JAN 73 1473

EDITION OF 1 NOV 65 IS OBSOLETE
S/N 0102-014-66011

UNCLASSIFIED

SECURITY CLASSIFICATION OF THIS PAGE (When Data Entered)

UNCLASSIFIED

SECURITY CLASSIFICATION OF THIS PAGE(When Data Entered)

In the cushion and the wave height distribution under the cushion appears to be modified from the encountered wave field primarily by the wave making effect of the bow and stern motion.

... - supplied page ...

17
Conf
1/11/1944



47

UNCLASSIFIED

SECURITY CLASSIFICATION OF THIS PAGE(When Data Entered)

LIST OF FIGURES

	Page
Figure 1 - Sketch of SES Model Including Bow and Stern Seal Configurations, and Midstation Sidewall Section	25
Figure 2 - Side View of Model and Towing Gear with Model Clear of Water	26
Figure 3 - Encountered Wave Spectra at 9 Knots, $F_n = 0.72$	27
Figure 4 - Encountered Wave Spectra at 12 Knots, $F_n = 0.96$	28
Figure 5 - Encountered Wave Spectra at 15 Knots, $F_n = 1.20$	29
Figure 6 - Cushion Pressure Response, $F_n = 0.72$, Significant Wave Height/Cushion Height = $\eta_{.392}$	30
Figure 7 - Cushion Pressure Response, $F_n = 0.72$, Significant Wave Height/Cushion Height = $\eta_{.529}$	31
Figure 8 - Cushion Pressure Response, $F_n = 0.96$, Significant Wave Height/Cushion Height = $\eta_{.309}$	32
Figure 9 - Cushion Pressure Response, $F_n = 0.96$, Significant Wave Height/Cushion Height = $\eta_{.693}$	33
Figure 10 - Cushion Pressure Response, $F_n = 1.20$, Significant Wave Height/Cushion Height = $\eta_{.267}$	34
Figure 11 - Heave Acceleration Response, $F_n = 0.72$, Significant Wave Height/Cushion Height = $\eta_{.392}$	35
Figure 12 - Heave Acceleration Response, $F_n = 0.72$, Significant Wave Height/Cushion Height = $\eta_{.529}$	36
Figure 13 - Heave Acceleration Response, $F_n = 0.96$, Significant Wave Height/Cushion Height = $\eta_{.309}$	37
Figure 14 - Heave Acceleration Response, $F_n = 0.96$, Significant Wave Height/Cushion Height = $\eta_{.693}$	38
Figure 15 - Heave Acceleration Response, $F_n = 1.20$, Significant Wave Height/Cushion Height = $\eta_{.267}$	39
Figure 16 - Heave Acceleration Transfer Functions in Regular and Irregular Waves, $F_n = 0.72$	40
Figure 17 - Heave Acceleration Transfer Functions in Regular and Irregular Waves, $F_n = 0.72$	41
Figure 18 - Heave Acceleration Transfer Functions in Regular and Irregular Waves, $F_n = 0.96$	42

LIST OF FIGURES (Cont'd)

	Page
Figure 19 - Heave Acceleration Transfer Functions in Regular and Irregular Waves, $F_n = 0.96$	43
Figure 20 - Heave Acceleration Transfer Functions in Regular and Irregular Waves, $F_n = 1.20$	44
Figure 21 - Wave Spectrum Variation, $F_n = 0.72$, Significant Wave Height/Cushion Height ⁿ = .392	45
Figure 22 - Wave Spectrum Variation, $F_n = 0.72$, Significant Wave Height/Cushion Height ⁿ = .529	46
Figure 23 - Wave Spectrum Variation, $F_n = 0.96$, Significant Wave Height/Cushion Height ⁿ = .309	47
Figure 24 - Wave Spectrum Variation, $F_n = 0.96$, Significant Wave Height/Cushion Height ⁿ = .693	48
Figure 25 - Wave Spectrum Variation, $F_n = 1.20$, Significant Wave Height/Cushion Height ⁿ = .267	49

NOMENCLATURE

B_c	Cushion beam
E	Area under the spectral curve
g	Gravitational constant
H_c	Cushion height
L_c	Cushion length
\tilde{P}	Gage pressure
PSFG	Pounds per square foot, gage
P	Normalized gage pressure
P_B	Gage pressure in forward region of the cushion
\tilde{P}_B	Normalized pressure in the forward region of the cushion
P_c	Spatial average cushion pressure
P_s	Gage pressure in stern region of the cushion
\tilde{P}_s	Normalized pressure in the stern region of the cushion
t	Time
U	Forward speed
X	Longitudinal coordinate, positive forward
z	Heave displacement
\ddot{z}	Heave acceleration
Δ	Craft weight
λ	Wavelength
ϵ	Constant to account for the fixed vertical position of the relative range sensors
ζ_a	Wave amplitude
θ	Pitch angle
ξ	Relative range between craft and water surface
η	Wave elevation

ABSTRACT

Mathematical models developed for air-cushion-supported vehicles generally approximate the air pressure as being uniformly distributed within the cushion of the vehicle and assume that the pressure has no effect on the encountered wave field. The validity of these approximations is examined experimentally by measuring the spatial and temporal distribution of the air pressure in and wave elevation under the cushion of a high length-to-beam ratio surface effect ship model which is free to heave and pitch in irregular head waves. It is observed that the pressure is distributed nonuniformly in the cushion and the wave height distribution under the cushion appears to be modified from the encountered wave field primarily by the wave making effect of the bow and stern motion.

ADMINISTRATIVE INFORMATION

This study was sponsored by the Naval Ship Systems Command and authorized under Task Area SF 4342170407, Work Unit Number 1-1507-200-34.

INTRODUCTION

The spatial variation of air pressure in the cushion of an air-cushion-supported vehicle (ACV) has generally been unaccounted for in the existing mathematical dynamic response models used to predict craft motions. Spatially uniform pressure distributions are the standard approximation. The temporal variation has been assumed to have a linear relationship to the craft motions or has been accepted as an independent variable in some formulations.

The effect of the increased pressure under an ACV on the incoming waves has been unknown heretofore and generally neglected in ACV dynamics. The standard assumption is that the waves pass under the vehicle without change in shape and emerge from the craft exactly as they entered, that is, the Froude-Kryloff hypothesis applied to ACV's.

The purpose of this investigation was to examine the effect of the cushion pressure distribution on the craft dynamic response and on the incident waves for a high length-to-beam (L/B) ratio surface effect ship (SES) in irregular waves. Previously, similar experimental results have been presented for the high L/B SES in regular waves by Moran^{1,2}(1975)*.

The data furnished by this experiment allows only for a basic examination of the spatial distribution of cushion air pressure. A justification for future, more extensive pressure mapping studies is given on the basis of these simple but conclusive pressure measurements. Complete spatial (and temporal) mappings, when available, would enable a detailed assessment of the interaction between the cushion air pressure, the craft dynamic response and the incident wave field.

* Superscripts refer to references on page .

The need for knowledge of the nature of the free surface under an ACV is found in the mathematical modeling of the craft and its dynamic characteristics in waves. Two important features of any dynamic model are the volume of air enclosed between the hard structure of the air-cushion-supported vehicle and the free surface; and the peripheral area between the seal structure of the vehicle and the free surface under the seals, commonly referred to as the leakage area. The behavior of the free surface in these regions must be known both in the temporal and spatial domains for prediction of craft operation in a wave field. Also it is of interest to know the free surface elevation in the cushion in order to predict the impacting of the hard structure and the water surface.

The free surface disturbance produced by a moving pressure field has been examined by a number of researchers. The two-dimensional solution to the problem of an oscillating pressure over a free surface has been examined by Wu³ (1957) and Kaplan⁴ (1957). Each formulation is concerned with the steady unidirectional motion of an oscillating two-dimensional pressure field in deep water. The problem of a stationary oscillating pressure field between side walls (two-dimensional) was also studied by Ogilvie⁵ (1969). Finite depth two-dimensional solutions have been examined by Debnath and Rosenblat⁶ (1969) through an extension of the deep water solutions. Most recently Doctors⁷ (1974) has presented a solution in three dimensions for an oscillating pressure field moving unidirectionally in an infinitely deep fluid. Doctors' three-dimensional solution allows the calculation of the free surface elevation within the cushion area (near field) and also predicts the radiated wave field (far field) for a given harmonic pressure disturbance. The solution is in

brief an extension of the DePrima and Wu⁸ (1957) two-dimensional solution to three dimensions. The analysis is a linearized irrotational flow model employing all of the usual linearizations and relies upon the introduction of an artificial (Rayleigh) viscosity to satisfy the radiation condition. The validity of Doctors' solution has not been verified experimentally and hence a second purpose of the present experimental program is to provide the beginning of a data base upon which analytic free surface models may be tested.

EXPERIMENTAL INVESTIGATION

Model Description

The high length-to-beam ratio surface effect ship used in the present experimental investigation was a 15 foot long model designated by the Naval Ship Research and Development Center as the XR-5. The model is shown schematically in profile in Figure 1. The flexible bow and stern seals are shown with their internal porous support membranes. The primary characteristics of the model are given in Table 1.

The model was constructed of polyurethane foam with a density of 9 pounds/feet³ and covered with a layer of fiberglass. The two sidewalls, with 45 degree deadrise (see Figure 1) and the bow and stern seals provided the peripheral air seal. Air was supplied to the plenum and seals by two stacked pairs of axial flow lift fans discharging into the bow seal and a similar set of two stacked pairs discharging into the stern seal. Cushion pressure was maintained by the air passing through the seals and into the cushion plenum.

The bow and stern seals consisted of three inflatable bags. Lift fan air was discharged into the two interconnected lower bags. The third, or upper, bag was inflated by opening a gate in a ducting network from the lower two

bags. The lower surface was a smooth curved semi-rigid planing surface. The upper and lower bags were enclosed by neoprene impregnated nylon which was fastened to the bottom of the model and the planing surface of the seal. The forward edge of the planing surface was hinged to the model.

A side view of the model mounted on the towing apparatus is shown in Figure 2. The towing frame is attached to the rear (East side) of Carriage 11 by means of an A-frame device. The pitch-heave towing gear from the Center's Tank at Langley Field, Virginia was mounted below the frame. The tow point was located forward of the model's longitudinal center of gravity (LCG) to ensure yaw stability. The tow cable was led through a sheave mounted to the heave staff to simulate a thrust axis along the lower edge of the keel. The model was free to pitch and heave. The model was fixed in surge by the tow cable, which was kept taut by applying a constant 20 pound force to the back of the surge roller cage using a force negator.

Instrumentation

The craft instrumentation consisted of pitch and heave transducers, wave height sensors, and cushion pressure transducers. The locations of all transducers are given in Table 2 with the positions referred to the model transom. The electronic characteristics of the rigid body and wave height transducers have been completely described by Moran¹ (1975).

The instrumentation for measuring cushion pressure was limited to two low-pressure transducers which were flush mounted on the upper surface of the craft plenum. Original plans for a complete pressure survey in the cushion were abandoned when mechanical failures severely limited the number of compatible pressure transducers available. The magnitude of the gage pressure in an ACV model cushion is extremely small. The average support pressure in

these model experiments was approximately .05 pounds per square inch. The accurate measurement of pressures of this magnitude, with harmonic content at frequencies up to 100 radians per second, requires extremely sensitive pressure transducers. Further, confidence in comparable pressure measurements (e.g., the difference between two small pressure signals for nearly the same magnitude) usually requires that the same type of pressure transducers be used for the measurements. In this investigation, a capacitance bridge pressure transducer was chosen for its high signal-to-noise ratio, low acceleration response, and good electronic stability. The pressure is measured through capacitance changes produced by the deflection of a thin membrane relative to a solid plate. This transducer is ideal for low pressure measurements in an air-cushion vehicle plenum because it couples a low pressure capability (0.2 psi maximum) with a high overload capability (100 psi maximum). The high overload capability is required since the pressure transducers are located in a region subject to wave impacts. The detailed mechanical and electrical properties of these transducers have been described by Moran² (1975).

The heaving and pitching motions of the craft were determined through linear potentiometers attached to the heave staff. The heave staff was unrestrained in vertical motion but the craft was not allowed to surge, yaw, sway, or roll. The location of the heave staff relative to the craft center of gravity is indicated in Table 2. A mechanical pulley system was employed to assure that the vertical position of the tow point was effectively located at the on-cushion static waterline.

Rigid body vertical accelerations were measured directly with two accelerometers attached to the model and located near the bow and at the center of gravity as indicated in Table 2.

The temporal variation of the free surface elevation was measured at six points along the centerline of the surface-effect ship model using Western Marine Electronics (WESMAR LM-4000) precision level monitors. The forwardmost sensor was attached to the rigid structure of the carriage. This sensor is referred to as the 'wave-height probe' and its location relative to the craft is indicated in Table 2. This probe was located sufficiently far ahead of the model that wave records were unaffected by the existence of the model downstream (in the direction of wave propagation). The other five sensors were mounted on the model along the longitudinal axis. The locations of these sensors relative to the craft transom are given in Table 2 where the sensors are designated as relative-range or sonic probes 1 through 5. Each of these transducers indicated as a function of time the relative distance (range) between the free surface and sensor which had a vertical motion due to the heaving and pitching motion of the model.

The ultrasonic relative-range transducers were mounted in pairs within the hard deck structure of the model. Two transducer units, a sending and a receiving unit, were necessary to allow measurement of elevations on the order of six to ten inches. The sending and receiving transducers were mounted side by side on a line perpendicular to the longitudinal axis of the craft and were canted at an angle of 8 degrees to the vertical so that they were focused on the mean water surface level for the craft underway. This configuration for the transducers minimized the number of dropout or lost **sonic** echo signals and in general produced a highly reliable system for measuring relatively large amplitude variations in elevation at close range.

Experimental Procedure

The experimental program was conducted at the Carriage II facility at the David W. Taylor Naval Ship Research and Development Center (DTNSRDC), Carderock, Maryland. The craft was free to heave and pitch in irregular waves at three speeds.

Before starting the random wave program, it was necessary to establish a representative operating condition for the craft. In particular, near-optimum fan configuration, duct valve settings and downstop settings had to be determined. This was done partly on the basis of earlier experimental data and from a series of exploratory random wave experiments in which the above parameters were adjusted to minimize motion. The duct valve settings for the reference model operating condition for the craft are given in Table 3. The reference fan arrangement was 2-0-2, i.e., two fans in the forward seal, none in the main plenum and two in the stern seal. The downstops were set in the maximum downward position. This operating condition is not necessarily the optimum one for the craft. It was impossible to explore all the combinations of operating conditions due to the time limitations; however, the reference condition is near-optimum from the seakeeping of ship motions standpoint, (as determined by Manguson⁹) while maintaining good drag and lift fan power characteristics. The reference condition is very close to the one selected in an earlier series of experiments where the effective horsepower (fan plus propulsion) was minimized.

The irregular seas experiment was designed to examine the behavior of the model in random waves whose encounter spectrum contained significant energy in the same range as the resonant frequencies of the model. The

experiments were carried out with the model on-cushion at 9, 12 and 15 knots, corresponding to Froude numbers of 0.72 (design speed), 0.96 and 1.20 (see Table 4). At 9 and 12 knots, runs were made in two sea states with similar frequency content but different significant wave heights.

The range of irregular wave conditions for the experiments is given in Table 5. Graphs of the wave spectra measured ahead of the model are in Figures 3 through 5. These particular spectra were chosen because of their significant energy content in the range of the resonant motion frequencies of the craft.

DATA ANALYSIS

The irregular sea data were recorded on magnetic tape and processed using a spectral analysis computer program. Data obtained in random waves were analyzed in both the time domain and the frequency domain. This analysis yields mean values, power spectra, histograms and Fourier transforms as well as statistical information about the time histories. The power spectra and transfer functions presented herein are obtained from auto-spectral analysis. The phase lag and the coherency data is a result of cross-spectral analysis. For the data concerning the two pressure measurements, the phase lag of the pressure at the stern P_S with respect to the pressure at the bow P_B is presented. For the acceleration data, the phase lag of the accelerometer measurement with respect to the pressure force is presented.

The acceleration presented as being determined from the pressure distribution is based on calculations discussed in detail by Moran²(1975). In short the vertical acceleration in g's was computed from

$$\ddot{z} = \frac{P_B L_c}{\Delta} \quad (1)$$

where P_c is a spatial average pressure computed from the pressure distribution, B_c is the cushion beam, L_c the cushion length and Δ the weight of the craft.

The wave elevation $\eta(x,t)$ at any longitudinal position x from the craft's center of gravity is obtained from the measured relative range (sonic probe output) and the craft's heaving and pitching motion according to

$$\eta(x,t) = z(t) - x\theta(t) - \xi(t) + \epsilon \quad (2)$$

where the heave is designated as $z(t)$, $\theta(t)$ is the pitch angle and $\xi(t)$ is the measured relative range between the craft and the water surface. The constant ϵ is included to account for the fixed vertical position of the relative range (sonic) sensors. It should be noted that the pitch angle $\theta(t)$ has been assumed to be small and hence all relative distances are taken as vertical and not inclined according to the craft's pitching attitude. The sign convention adopted for the heave signal is positive upward and the pitch angle is positive for a bow down attitude. The longitudinal coordinate x is accordingly positive in the forward direction.

EXPERIMENTAL RESULTS

The discussion of the experimental results is divided into three sections: pressure distribution, exciting force and free surface deformation.

Pressure Distribution

Figures 6 through 10 present the results of spectral analysis of the two cushion pressure measurements. The pressure transfer functions \tilde{P} are non-dimensionalized as

$$\tilde{P} = \frac{P_c B_c L_c H_c}{\zeta_a \Delta}$$

where H_c is the cushion height and ζ_a is the wave amplitude (the others were defined previously). The subscripts in the figures refer to the cushion locations near the bow (B) and the stern (S) of the model, not to the seals.

All the data exhibit a common trait, that of distinct frequencies where the two signals become incoherent due to inversions in the phase. The low frequency incoherencies occur at a wavelength to cushion length ratio of approximately 1.10 for all three speeds. The secondary **incoherency**, although only shown in the figures for the lowest speed, occurs at a wavelength to cushion length ratio of 0.55. These distinct incoherencies are an indication that a definite frequency dependence exists in the pressure distribution mechanism of the XR-5 model. A listing of these null points is presented in Table 6. It can be shown theoretically that for regular waves, null points in the craft responses due to geometrical wave pumping exist at wavelength to ship length ratios of 1, 1/2, 1/3 etc. which correspond to these incoherencies.

Likewise, examination of nondimensional pressure transfer functions tends to support the contention that the spatial distribution of pressure in the cushion is nonuniform. It appears that the pressure variations near the bow are much greater than those near the stern for the lower frequencies; however the situation is reversed at the higher frequencies. This may be due to the bow seal responding to the pitching motion of the craft and affecting the pressure near the bow. The pressure near the stern appears influenced by the action of the stern seal which is possibly activated more by heaving than pitching.

Excitation Force

Data relating to the investigation of the heave excitation force are presented in Figures 11 through 20. In the first five figures, measured acceleration is compared to that computed from the pressure distribution using Equation 1. (In

actuality, it is a pressure force nondimensionalized by the model weight).

Several definite trends are observed. First, as expected, the acceleration and the nondimensional pressure force are very much in phase. Secondly, distinct incoherencies occur at the same frequencies as the pressure measurements although not as severe, i.e. at wavelengths of approximately 1.1 cushion lengths. Lastly, the transfer functions reach their maxima at frequencies corresponding to the natural pitch period of the craft. Secondary peaks in the transfer functions generally appear at the frequencies where wave pumping occurs. These secondary peaks are more distinct for the lower sea conditions investigated. A third peak exists in the nine knots data at a frequency corresponding to the distinct high frequency incoherency.

The second set of five graphs, Figures 16 through 20, presents comparisons of acceleration transfer functions computed from the spectral analysis of the irregular wave experimental data with the first harmonic component results from a series of regular wave experiments by Moran² (1975). The acceleration computed from the pressure distribution was calculated by Equation 1. In general, in the lower frequency range correlation is as good between regular wave and irregular wave accelerometer measurements as it is between irregular wave accelerometer measurements and predictions based on irregular wave pressure distributions. Some reasonable correlation with the predictions based on regular wave pressure distributions at the lower frequencies is seen. Little correlation could be found for any of the quantities in the higher frequencies although little model data was available for those frequencies. As mentioned earlier, null points in the acceleration exist for regular waves of wavelength to ship length ratios of 1, 1/2, 1/3 etc; however these particular waves were not examined in the regular wave experiments to determine how low the response would become.

The pitch exciting moment due to the varying pressure distribution was examined for irregular waves similar to the examination for regular waves by Moran²(1975). No discernable trends were evident, possibly due to the limited number of measurements used to define the cushion pressure distribution; hence no pitch moment data is included in this presentation.

Free Surface Deformation

The effect of the craft motion and the cushion pressure on the incident waves spectra is presented in Figures 21 through 25, and Table 7. It appears that the craft is adding energy to the incoming waves. The solid line labelled "forward of model" corresponds to the data presented in Figures 3 through 5. The symbol-lines labelled "bow" and "stern" are locations just forward and aft of the model. The other symbol-lines are described with respect to their relative locations in the cushion. These locations are not symmetric with respect to any definite location. The actual locations are listed in Table 2.

Examination of the data reveals that the most energy is being added to the incoming wave spectra near the forward cushion area in the frequency range of the modal wave frequency. Previously Figures 6 through 10 indicated that the cushion pressure variation is much greater near the bow than near the stern for the lower frequencies.

Significant energy remains in the waves exiting the craft as seen by the measurements at the stern. Considerable energy addition is also seen at the aft cushion location, and at the location just forward of the model.

Table 7 gives a further indication of the energy added to the incoming waves. Data are presented as ratios of the significant wave height at the point indicated to the significant wave height far forward of the model. The increase

in the significant wave height forward of the bow of the craft (denoted as BOW) is due to the unsteady wave generation of the relative motion of the bow seal. For unsteady operation, waves propagate ahead of the craft and are therefore detected as additional excitation superposed on the ambient irregular wave field. The major increase in wave energy under the craft is aft of the bow seal and is caused by the combined effects of bow seal motion, sidehull wave generation, wave generation by the unsteady cushion pressure and the increased wave field produced by the forward moving unsteady bow waves noted previously.

Near the longitudinal center of the cushion the relative motion is small and the wave field is increased only slightly above the ambient sea. In the mid cushion, the cushion pressure varies less than at the bow and stern and the sidehulls are ineffective wave generators (for internal waves) compared with the bow and stern seals. Small values of significant wave height in the mid cushion may also be caused by an apparent wave interference mechanism detected by Moran² in the regular wave experiments with the same model. Finally, the large values of significant wave height measured near the stern of the craft are caused by the significant relative stern motion and the dynamic response character of the planing stern seal in contact with the water surface.

CONCLUSIONS

Experimental results for a high length-to-beam ratio surface-effect ship operating dynamically in irregular head seas indicate that the cushion pressure is spatially inhomogeneous for unsteady-irregular excitation. The magnitudes and phase angles of the cushion pressure transfer functions measured at separate points in the cushion vary with frequency. The phase lag between pressures

exhibits half cycle variations over the encounter frequency range examined.

The magnitude of the pressure transfer function is observed to be greater at the bow than at the stern for low frequency excitation. In general this trend is found to be reversed for high frequency encounters.

The vertical acceleration of the craft has been found to be well correlated with the cushion pressure. The two variables are seen to be in phase over the entire encounter frequency domain. The peaking characteristics of the transfer functions relating acceleration and pressure imply the importance of the sidewall contribution to the vertical forcing function as compared to dominant contribution of the cushion dynamics.

The irregular-sea heave-acceleration transfer functions compare reasonably well at low frequencies with results obtained in regular waves. However, the vertical accelerations computed from regular wave pressure measurements fall below the corresponding irregular sea results at low frequencies. The acceleration null point implied in the regular wave experiments for wave lengths equal to the cushion length is also apparent in the irregular wave results however the double peak character is not as distinct for irregular wave excitation.

The surface wave spectra measured at six longitudinal positions along the centerline of the craft are all of similar form. The experimental results imply that the craft is adding energy to the encountered wave field through craft generated waves. These waves which are produced by the vertical motion of the sidehulls, seals and the spatial and temporal variations in cushion pressure are superposed on the ambient sea. The increase in energy of the measured spectra has been indicated through a presentation of the significant wave height determined from the measured wave spectra.

ACKNOWLEDGMENTS

The authors would like to express their appreciation to the Surface Effect Ship Division of the Aviation and Surface Effects Department, Naval Ship Research and Development Center for the use of the XR-5 surface-effect ship model tested under this program.

The personnel associated with the test program deserve special notice. James A. Kallio, James A. Fein and Allen H. Magnuson were jointly responsible for the performance of the test program. J. Brooks Peters was responsible for most of the final data analysis and preparation.

REFERENCES

1. Moran, D.D., "The Wave Height Under a High Length-to-Beam Ratio Surface-Effect Ship in Regular Waves", Ship Performance Department Report SPD 587-01, May 1975
2. Moran, D.D., "Cushion Pressure Properties of a High Length-to-Beam Ratio Surface Effect Ship", Ship Performance Department Report SPD 600-01, May 1975
3. Wu, T.Y.-T., "Water Waves Generated by the Translatory and Oscillatory Surface Disturbance", California Institute of Technology Engineering Division Report No. 85-3 (July 1957)
4. Kaplan, P., "The Waves Generated by the Forward Motion of an Oscillatory Pressure Distribution," Proceedings of the Fifth Midwestern Conference on Fluid Mechanics, Ann Arbor, Michigan (1957)
5. Ogilvie, T.F., "Oscillating Pressure Fields on a Free Surface", The University of Michigan, Department of Naval Architecture and Marine Engineering, Report No. 030 (September 1969).
6. Debnath, L., and S. Rosenblat, "The Ultimate Approach to the Steady State in the Generation of Waves on a Running Stream", Quarterly Journal of Mechanics and Applied Mathematics, Vol. 22, Part 3 (1969)
7. Doctors, L.J., "The Hydrodynamic Influence on the Nonlinear Motion of an Air-Cushion Vehicle over Waves", Proceedings of the Tenth Symposium on Naval Hydrodynamics, Cambridge, Massachusetts (June 1974)
8. DePrima, C.R., and T.Y.-T. Wu, "On the Theory of Surface Waves in Water Generated by Moving Disturbances", California Institute of Technology, Engineering Division, Report No. 21-23 (May 1957).
9. Magnuson, A.H., and K.K. Wolff, "Seakeeping Characteristics of the XR-5, A High Length-Beam Ratio Manned Surface Effect Testcraft: II. Results of Linearity Investigation, Effects of Changes from Reference Operating Condition and Trim and Draft in Regular Waves", SPD 616-02, March 1975.

TABLE 1
HIGH L/B SES MODEL CHARACTERISTICS

<u>Symbol</u>		<u>Dimensions Model Scale</u>	
LOA	Length Overall	15.58 ft	4.75 m
-	Design Displacement	275.0 lbs	124.74 kg
-	Test Displacement	298.0 lbs	135.17 kg
L	Length of Bubble	13.83 ft	4.22 m
B	Beam of Bubble	2.12 ft	0.65 m
L/B	Ratio	6.54	6.54
TCG	Transverse Center of Gravity	E	E
VCG	Vertical Center of Gravity (Above Keel Line)	0.90 ft	0.27 m
LCG	Longitudinal Center of Gravity (Forward of Transom)	7.21 ft	2.20 m
K	Radius of Gyration (in Pitch)	4.71 ft	1.44 m
K/LOA	Ratio	0.30	0.30
	Tow Point Forward of Transom	9.63 ft	2.94 m
	Tow Point Above Keel Line	0.97 ft	0.30 m

TABLE 2
TRANSDUCER LOCATIONS ON MODEL

<u>Transducer or Reference Point</u>	<u>Forward of the Transom</u>	
	<u>Feet</u>	<u>Meters</u>
Wave Height Probe (Carriage Borne)	51.125	15.583
Relative-Range (Sonic) Probe #1 (RBM)	15.911	4.850
Bow	15.580	4.749
Trailing Edge of Bow Seal	14.163	4.317
Relative-Range (Sonic) Probe #2	13.109	3.996
Pitch Heave Staff	9.625	2.934
Relative-Range (Sonic) Probe #3	7.974	2.430
Longitudinal Center of Gravity	7.208	2.197
Relative-Range (Sonic) Probe #4	2.588	0.789
Trailing Edge of Stern Seal	0.333	0.102
Transom	0	0
Relative-Range (Sonic) Probe #5 (RSM)	-0.229	-0.070

TABLE 3
OPERATING CONDITIONS FOR MODEL

Fan Configuration: 2-0-2 (Two fans in forward seal, none in main plenum, and two in stern seal)

Downstop Settings: All Downstops at maximum downward position

Duct Valve Settings: (Orifice Areas)

Main Bow Seal	4 in ²	25.81 cm ²
Third Lobe, Bow	0.625 in ²	4.03 cm ²
Main Stern Seal	5.5 in ²	35.49 cm ²
Third Lobe, Stern	4 in ²	25.81 cm ²

TABLE 4

SPEED IN KNOTS FOR VARIOUS SCALE RATIOS
OF XR-5 HIGH L/B SES, AS A FUNCTION
OF FROUDE NUMBER

$$F_n = \frac{U}{\sqrt{gL}}$$

	Tow Tank Model (Scale ratio = 1/3)	Manned Testcraft (Scale ratio = 1)	Proposed Ship (Scale ratio = 10.667)
0.48	6	10.4	40
0.72	9	15.6	51
0.96	12	20.8	68
1.20	15	26.0	85

TABLE 5
SUMMARY OF RANDOM WAVE CONDITIONS

XR-5 Model
Head Seas

MODEL SPEED (KNOTS)	SIGNIFICANT* WAVE HEIGHT	MEAN TRIM BOW UP (DEGREES)	MEAN SINKAGE (FEET)	MEAN CUSHION PRESSURE NEAR BOW (PSFG)	MEAN CUSHION PRESSURE NEAR STERN (PSFG)
9	.286	2.19	.320	8.40	8.30
9	.386	2.17	.363	7.53	7.48
12	.225	2.32	.302	8.53	8.37
12	.505	2.20	.399	7.03	6.03
15	.195	2.30	.342	8.18	7.89

MODEL SPEED (KNOTS)	SIGNIFICANT* WAVE HEIGHT (METERS)	CYCLES OF WAVES ENCOUNTERED	MEAN CUSHION PRESSURE NEAR BOW (PASCALS GAGE)	MEAN CUSHION PRESSURE NEAR STERN (PASCALS GAGE)
9	.087	167	402.2	397.4
9	.118	246	360.5	258.1
12	.069	302	408.4	400.8
12	.154	202	336.6	288.7
15	.059	138	391.7	377.8

*Significant Value = $4.00 \sqrt{E}$

TABLE 6
CHARACTERISTICS NULL POINTS

MODEL SPEED (KNOTS)	FROUDE NUMBER (U/\sqrt{gL})	WAVELENGTH CUSHION LENGTH (λ/L)	WAVE FREQUENCY (Radians/Second)	ENCOUNTER FREQUENCY (Radians/Second)
9	0.72	1.10	3.64	9.91
		0.55	5.15	17.69
12	0.96	1.10	3.64	12.00
		0.55	5.15	21.87
15	1.20	1.10	3.64	14.10
		0.55	5.15	26.06

TABLE 7

SIGNIFICANT WAVE HEIGHTS
NEAR AND BELOW THE MODEL

FROUDE NUMBER	SIGNIFICANT WAVE HEIGHT FWD OF MODEL		SIGNIFICANT WAVE HEIGHT/SIGNIFICANT WAVE HT FWD OF MODEL				
	CUSHION HEIGHT	HEIGHT	BOW	FWD CUSHION	MID CUSHION	AFT CUSHION	STERN
0.72	0.392		1.41	1.72	1.39	1.55	1.63
0.72	0.529		1.20	1.48	1.04	1.26	1.38
0.96	0.309		1.10	1.49	1.15	1.11	1.52
0.96	0.693		1.19	1.50	1.11	1.06	1.30
1.20	0.267		1.07	-	1.17	1.05	1.41

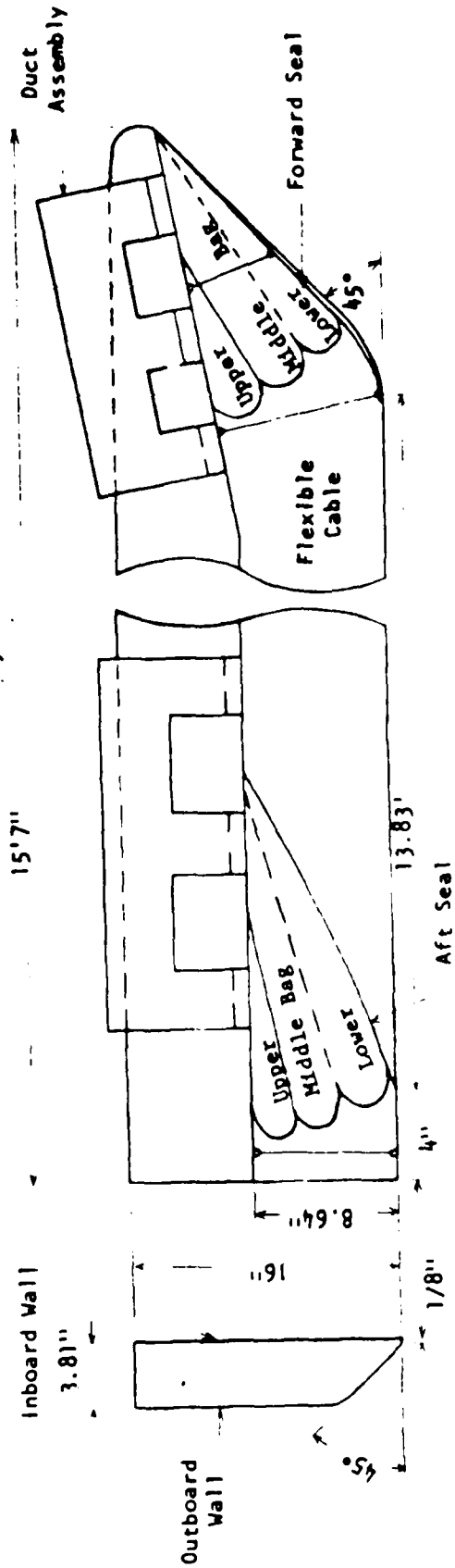


Figure 1 - Sketch of SES Model Including Bow and Stern Seal Configurations, and Midstation Sidewall Section

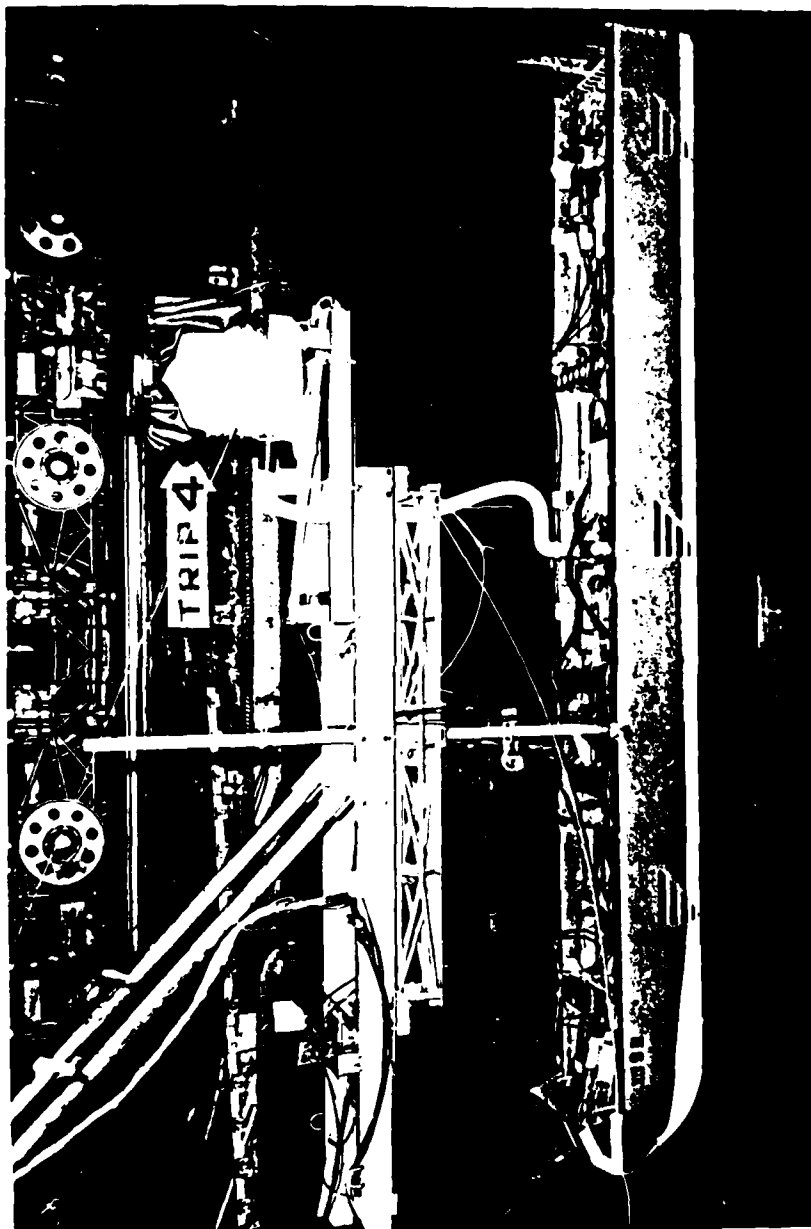


Figure 2 - Side View of Model and Towing Gear Showing
Model Hoisted Clear of Water

XR-5 Model

9 Knots

Head Seas

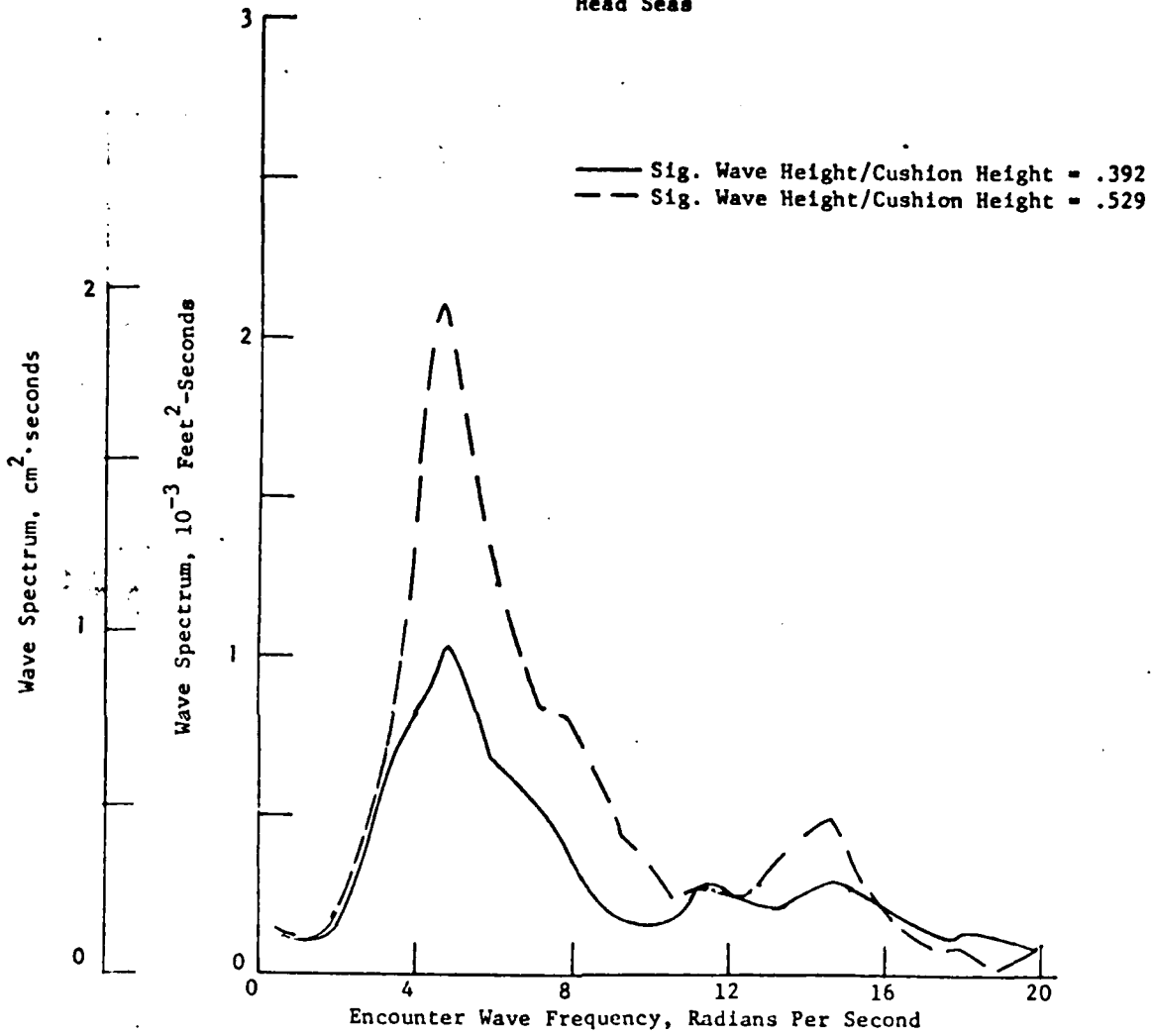


Figure 3 - Encountered Wave Spectra at 9 Knots, $F_n = 0.72$

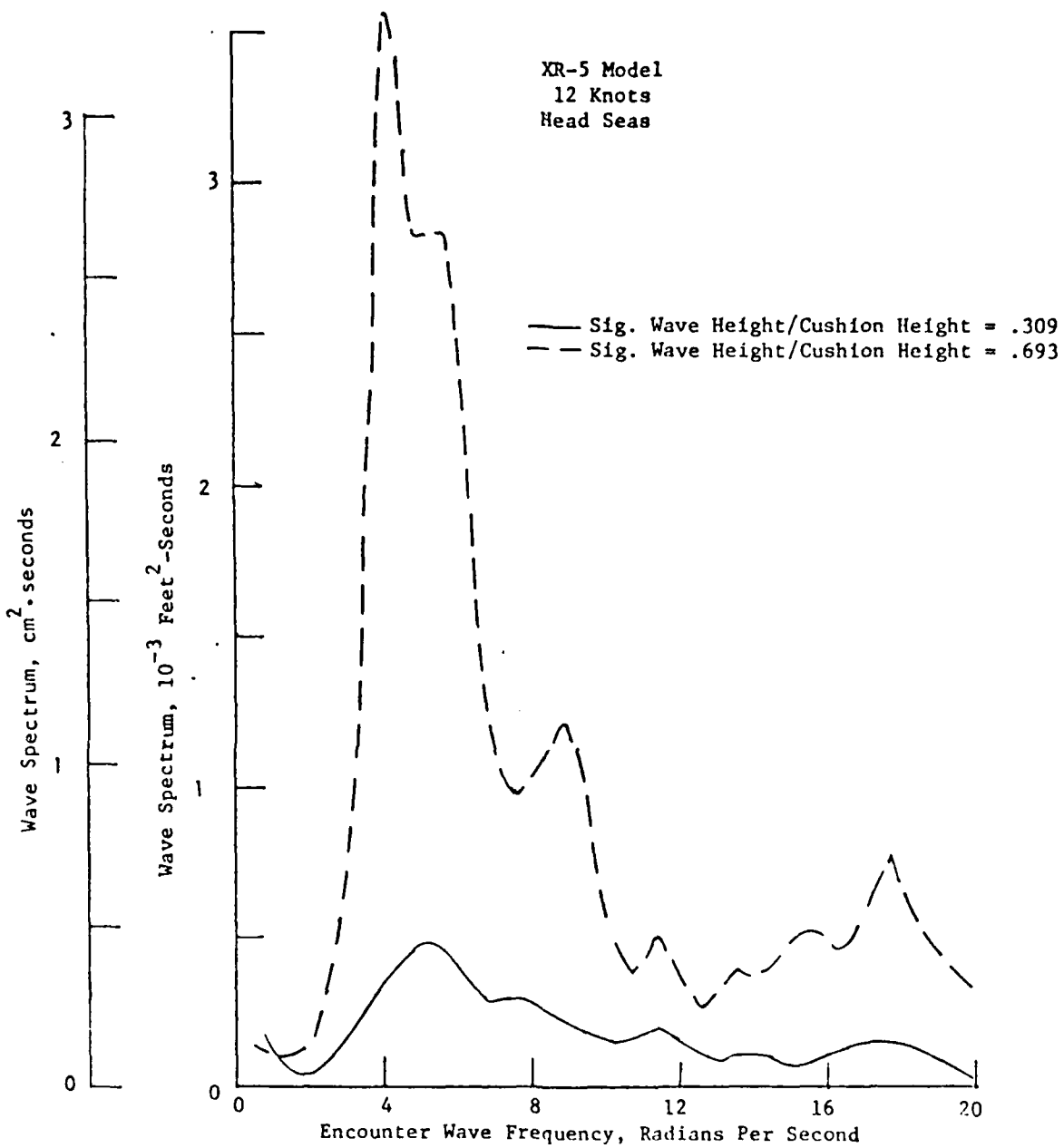


Figure 4 - Encountered Wave Spectra at 12 Knots, $F_n = 0.96$

XR-5 Model
15 Knots
Head Seas

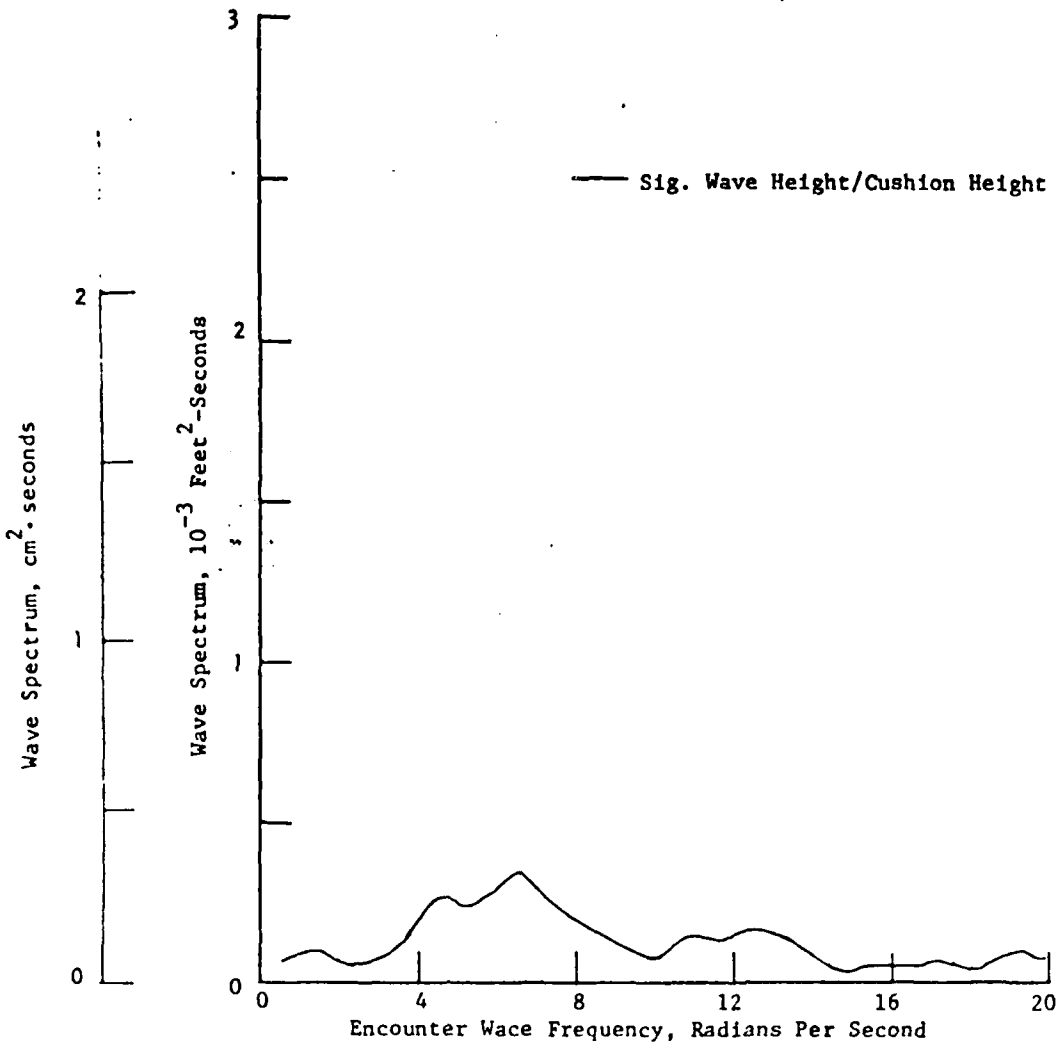


Figure 5 - Encountered Wave Spectra at 15 Knots, $F_n = 1.20$

XR-5 Model

$F_n = 0.72$

$\frac{\text{Significant Wave Height}}{\text{Cushion Height}} = 0.392$

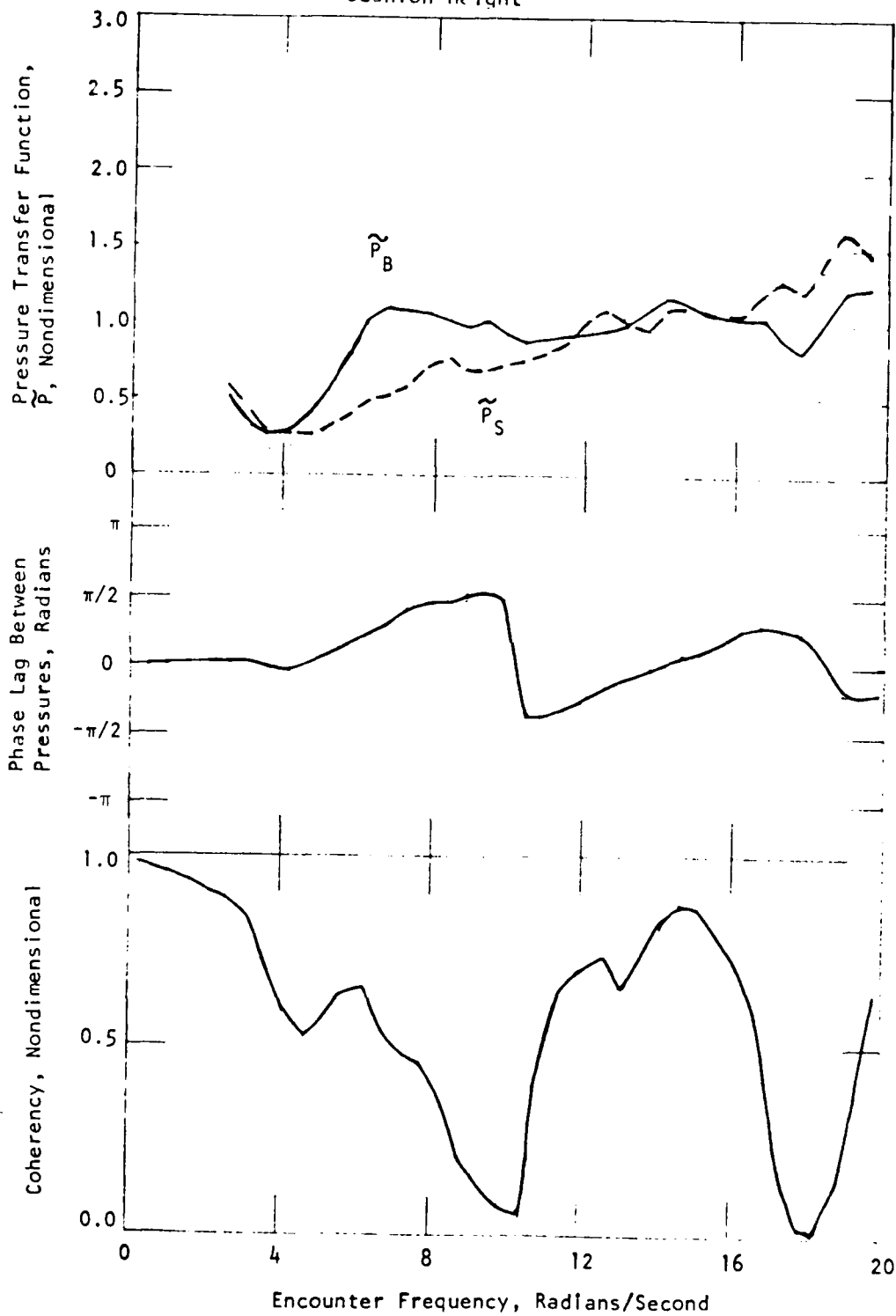


Figure 6 - Cushion Pressure Response, $F_n = 0.72$, Significant Wave Height/Cushion Height = 0.392

XR-5 Model
 $F_n = 0.72$

$\frac{\text{Significant Wave Height}}{\text{Cushion Height}} = 0.529$

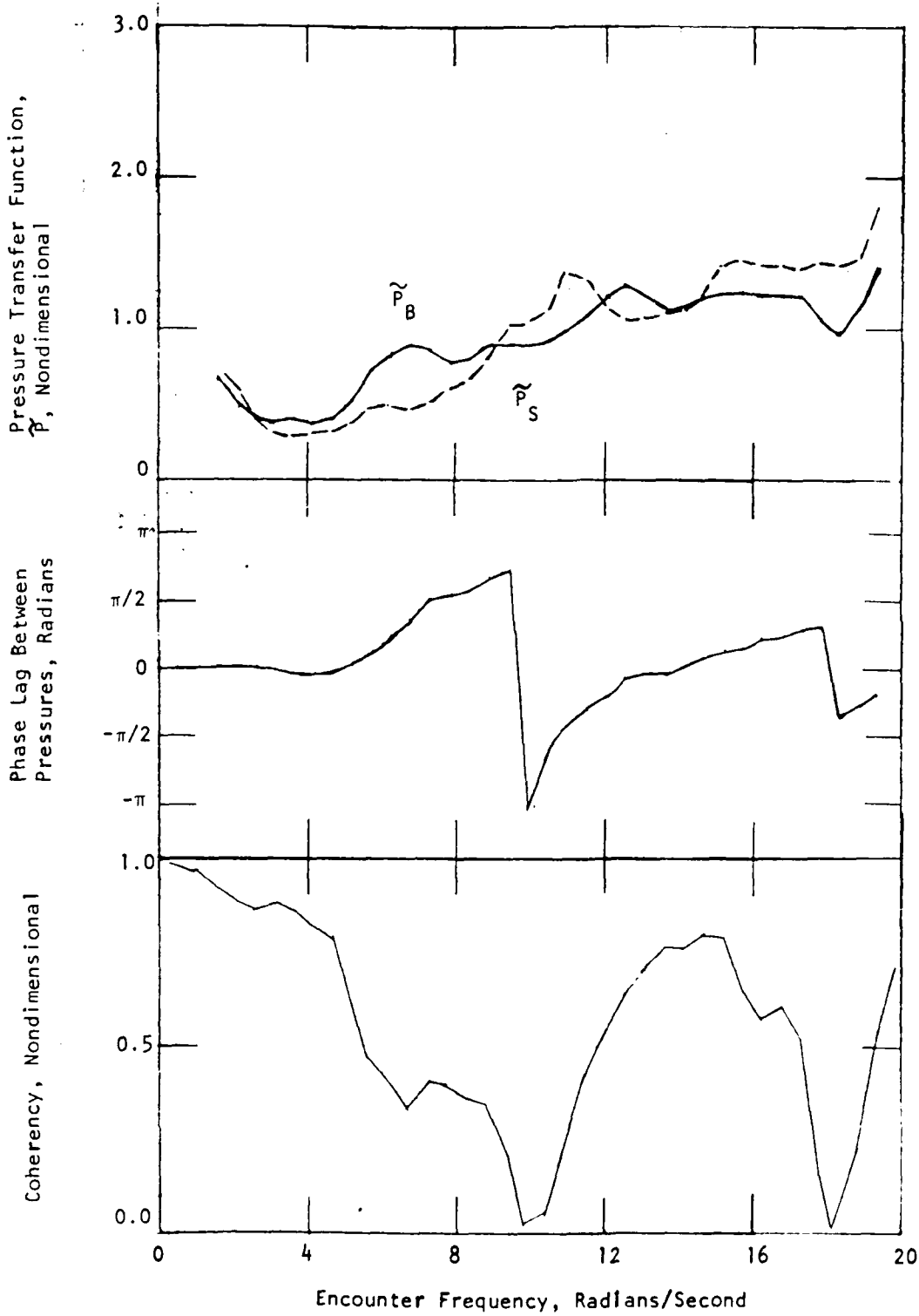


Figure 7 - Cushion Pressure Response, $F_n = 0.72$, Significant Wave Height/Cushion Height = 0.529

XR-5 Model
 $F_n = 0.96$

Significant Wave Height / Cushion Height = 0.309

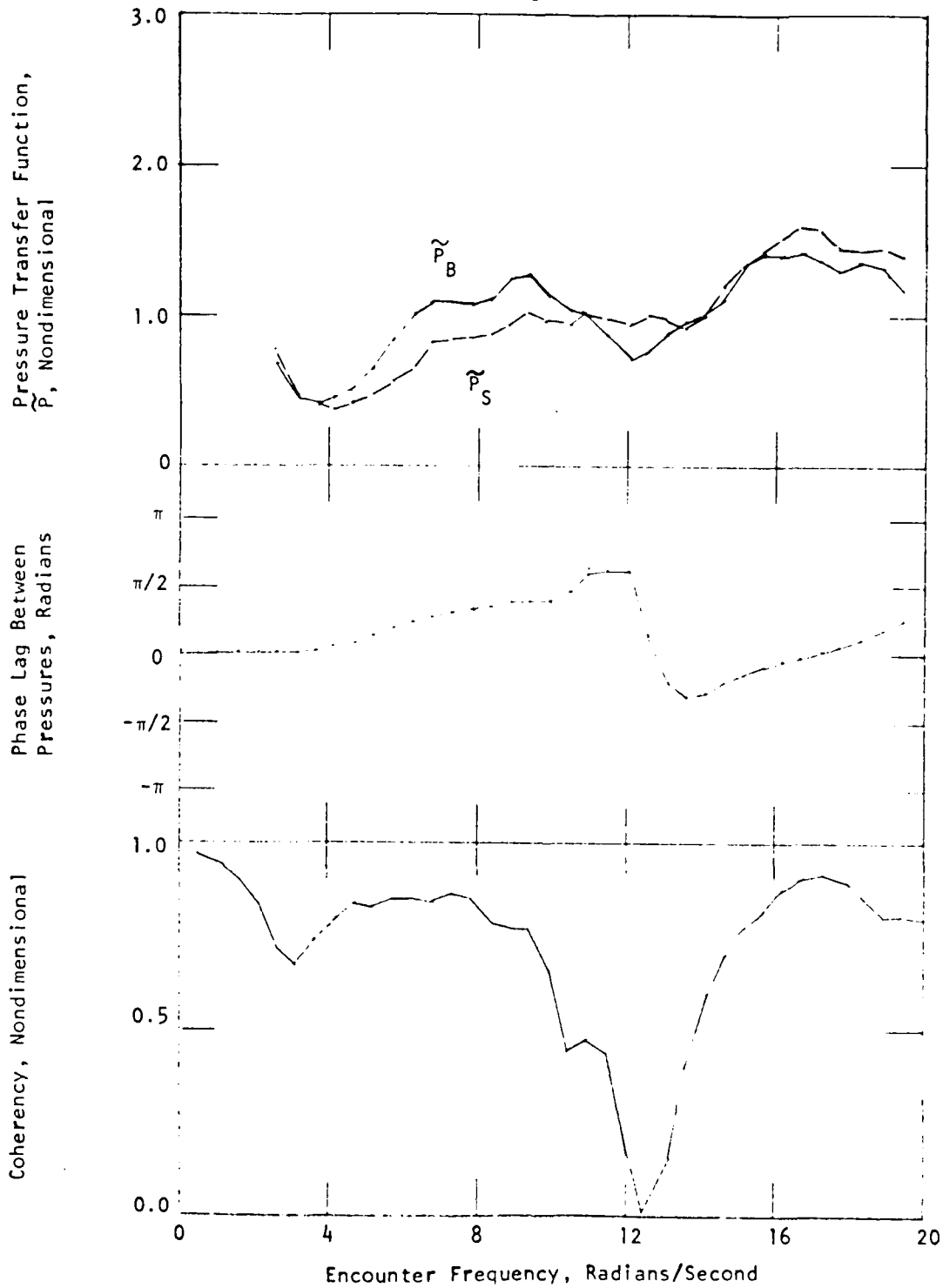


Figure 8 - Cushion Pressure Response, $F_n = 0.96$, Significant Wave Height/Cushion Height = 0.309

XR-5 Model
 $F_n = 0.96$

$\frac{\text{Significant Wave Height}}{\text{Cushion Height}} = 0.693$

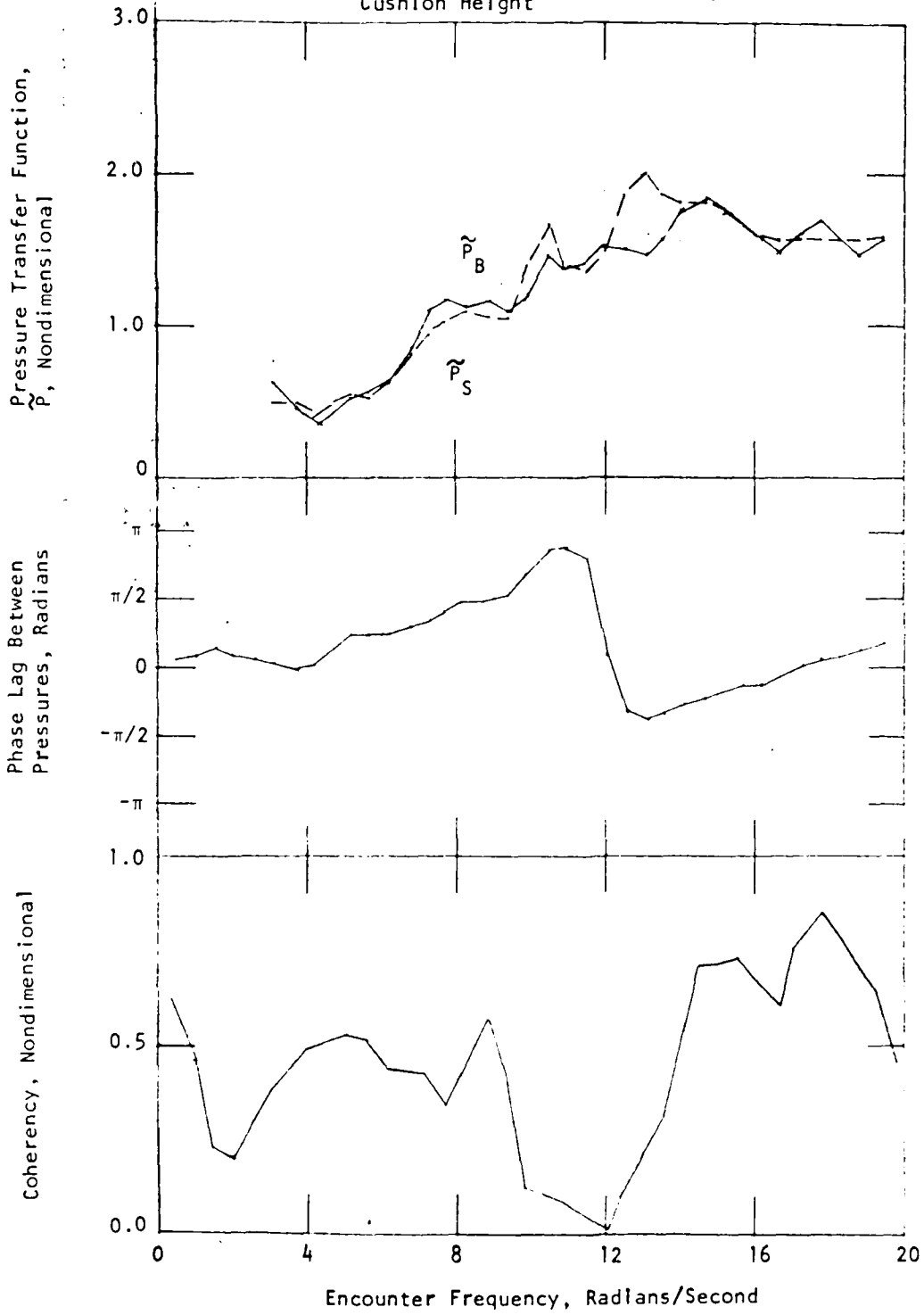


Figure 9 - Cushion Pressure Response, $F_n = 0.96$, Significant Wave Height/Cushion Height = 0.693

XR-5 Model
 $F_n = 1.20$

Significant Wave Height = 0.267
Cushion Height

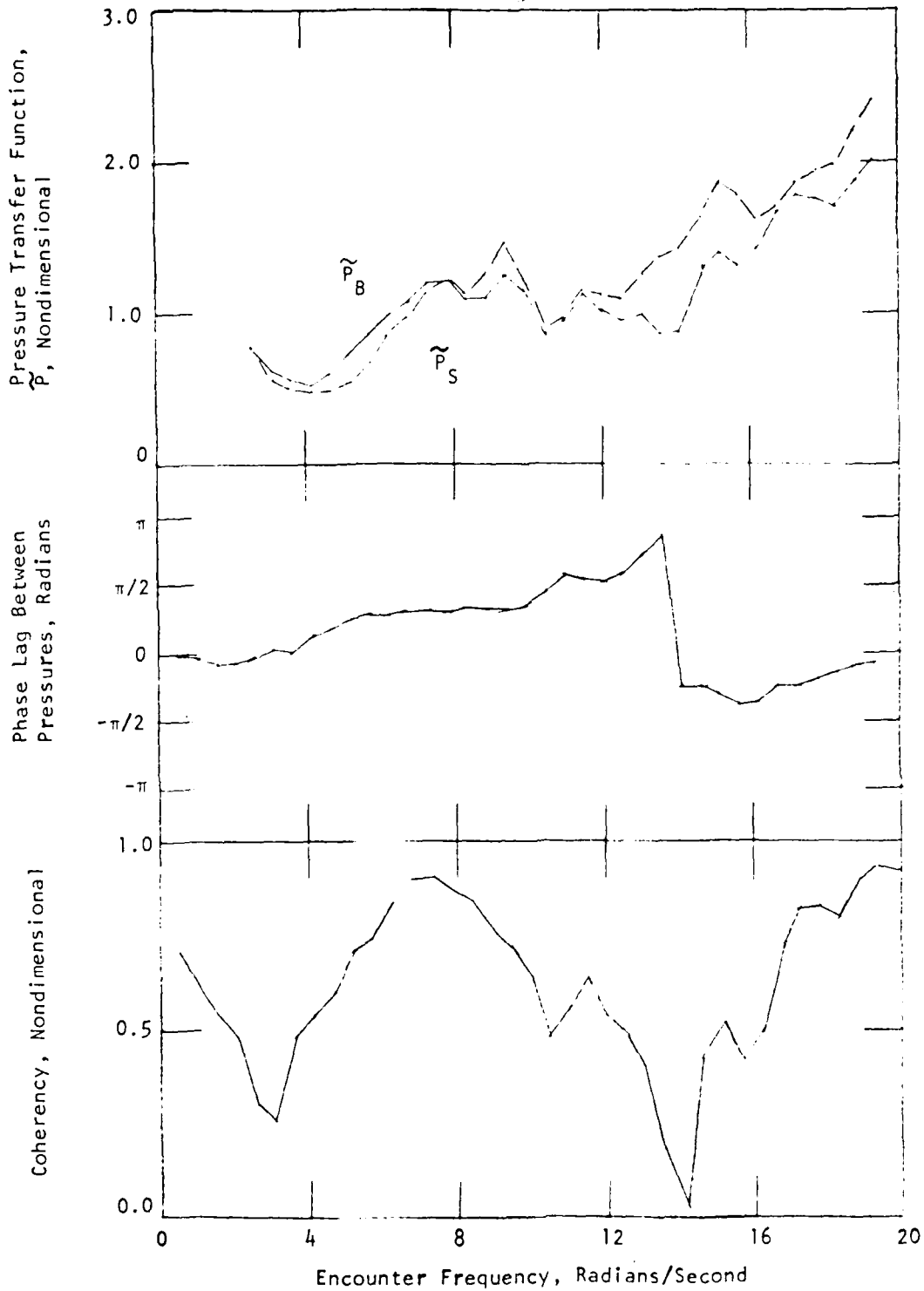


Figure 10 - Cushion Pressure Response, $F_n = 1.20$, Significant Wave Height/Cushion Height = .267

Accelerometer Measurement/Pressure Distribution Calculation

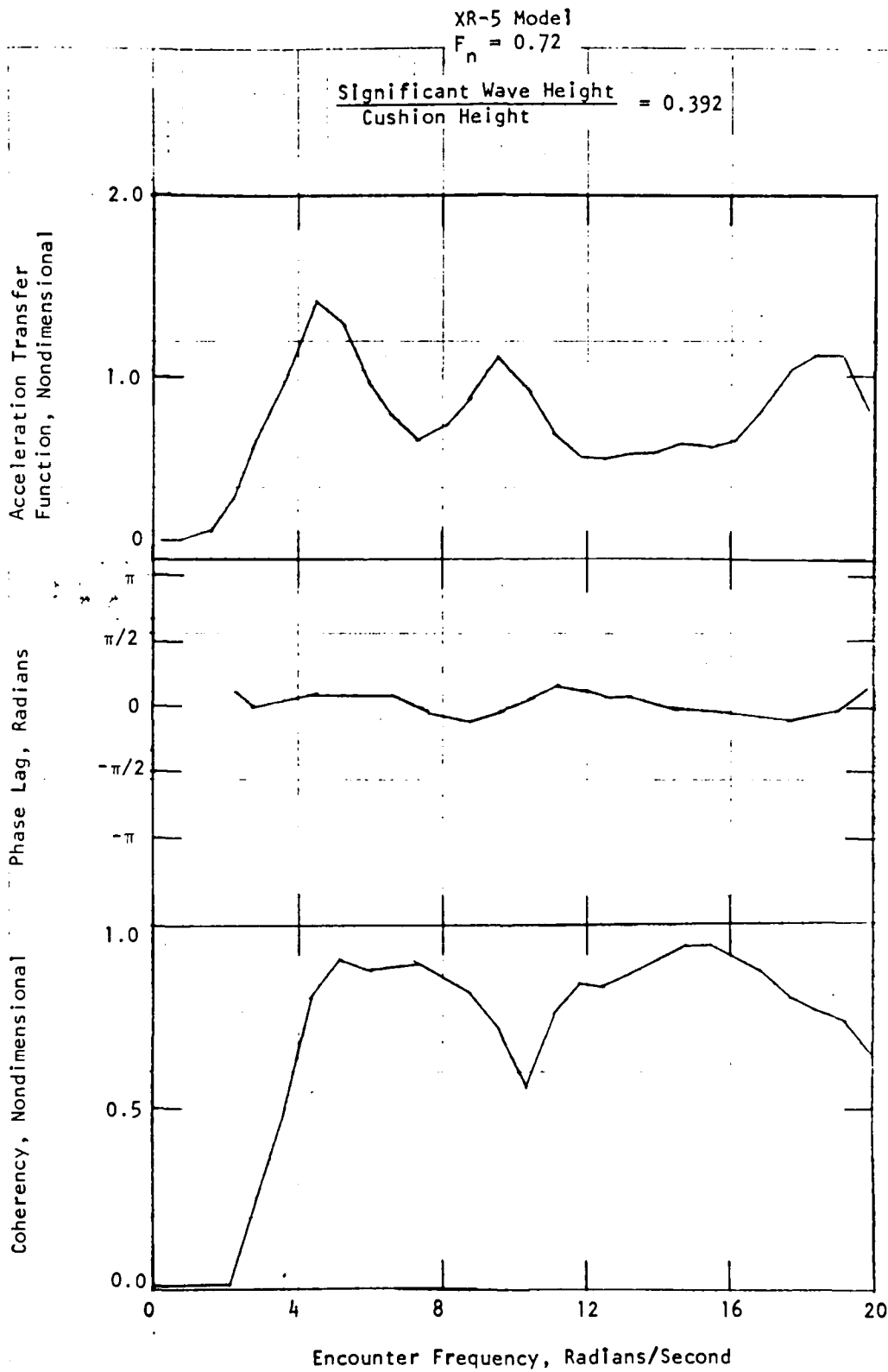


Figure 11 - Heave Acceleration Response, $F_n = 0.72$, Significant Wave Height/Cushion Height = 0.392

Accelerometer Measurement/Pressure Distribution Calculation

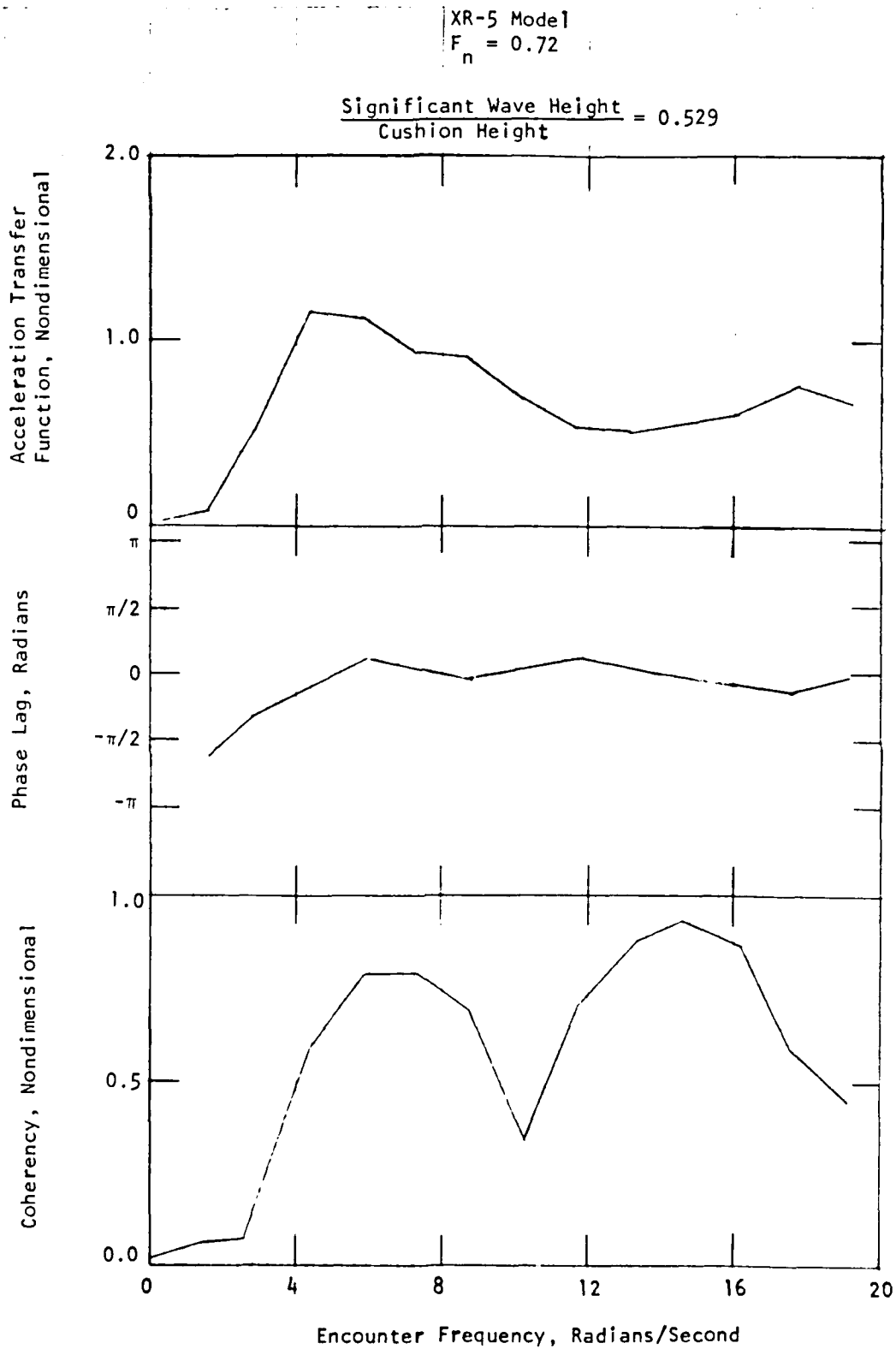


Figure 12 - Heave Acceleration Response, $F_n = 0.72$, Significant Wave Height/Cushion Height = 0.529

Accelerometer Measurement/Pressure Distribution Calculation

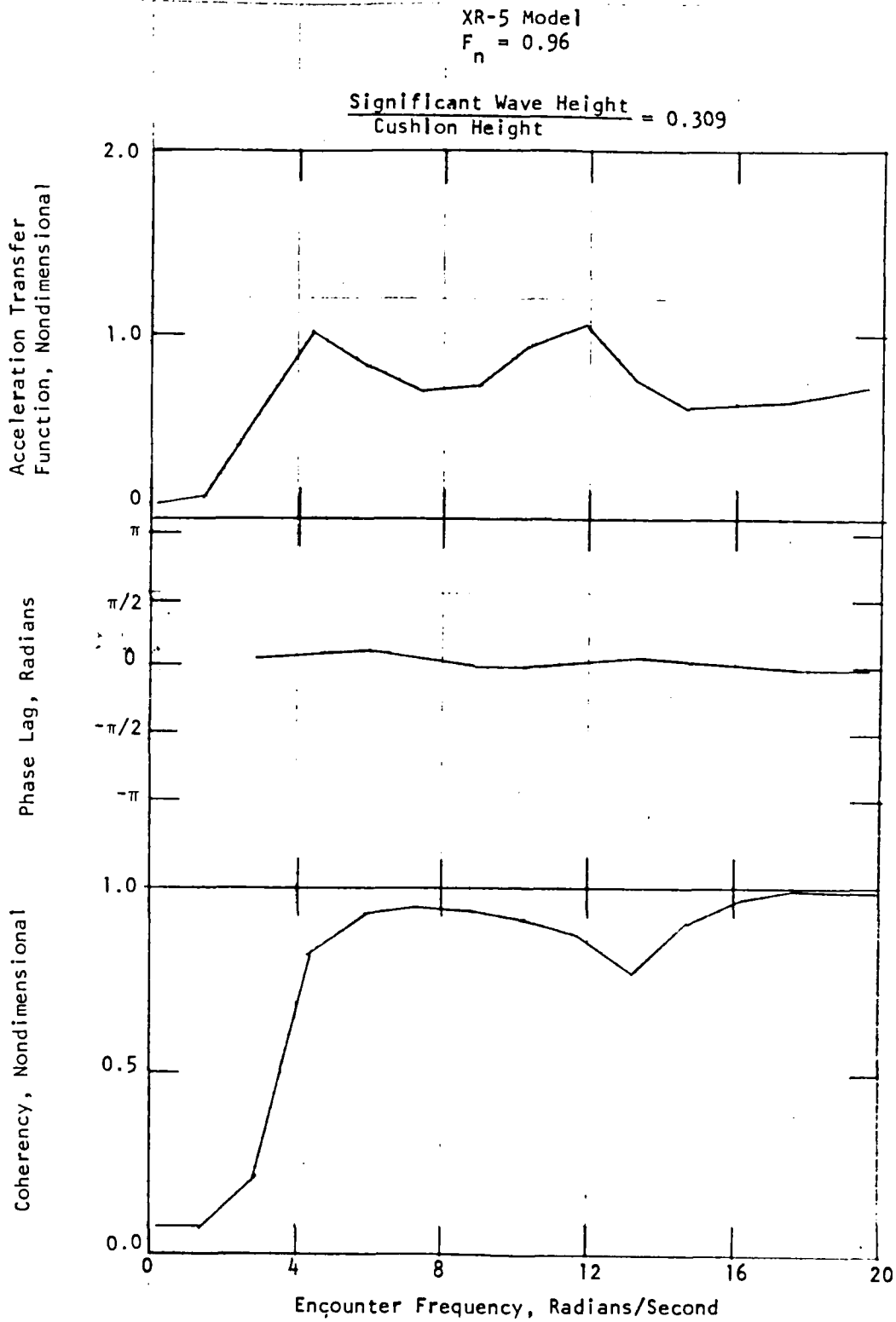


Figure 13 - Heave Acceleration Response, $F_n = 0.96$, Significant Wave Height/Cushion Height = 0.309

Accelerometer Measurement/Pressure Distribution Calculation

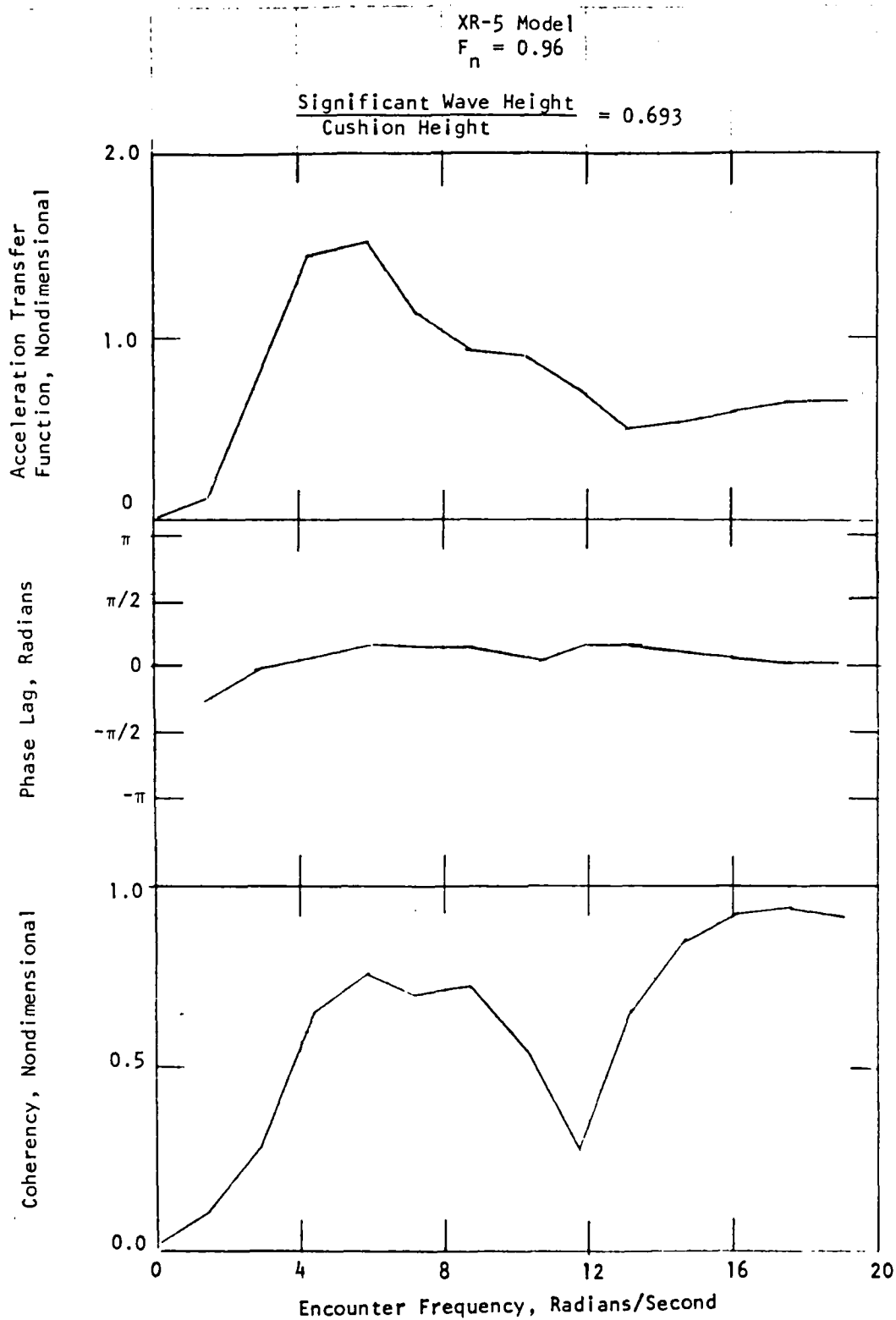


Figure 14 - Heave Acceleration Response, $F_n = 0.96$, Significant Wave Height/Cushion Height = 0.693

Accelerometer Measurement/Pressure Distribution Calculation

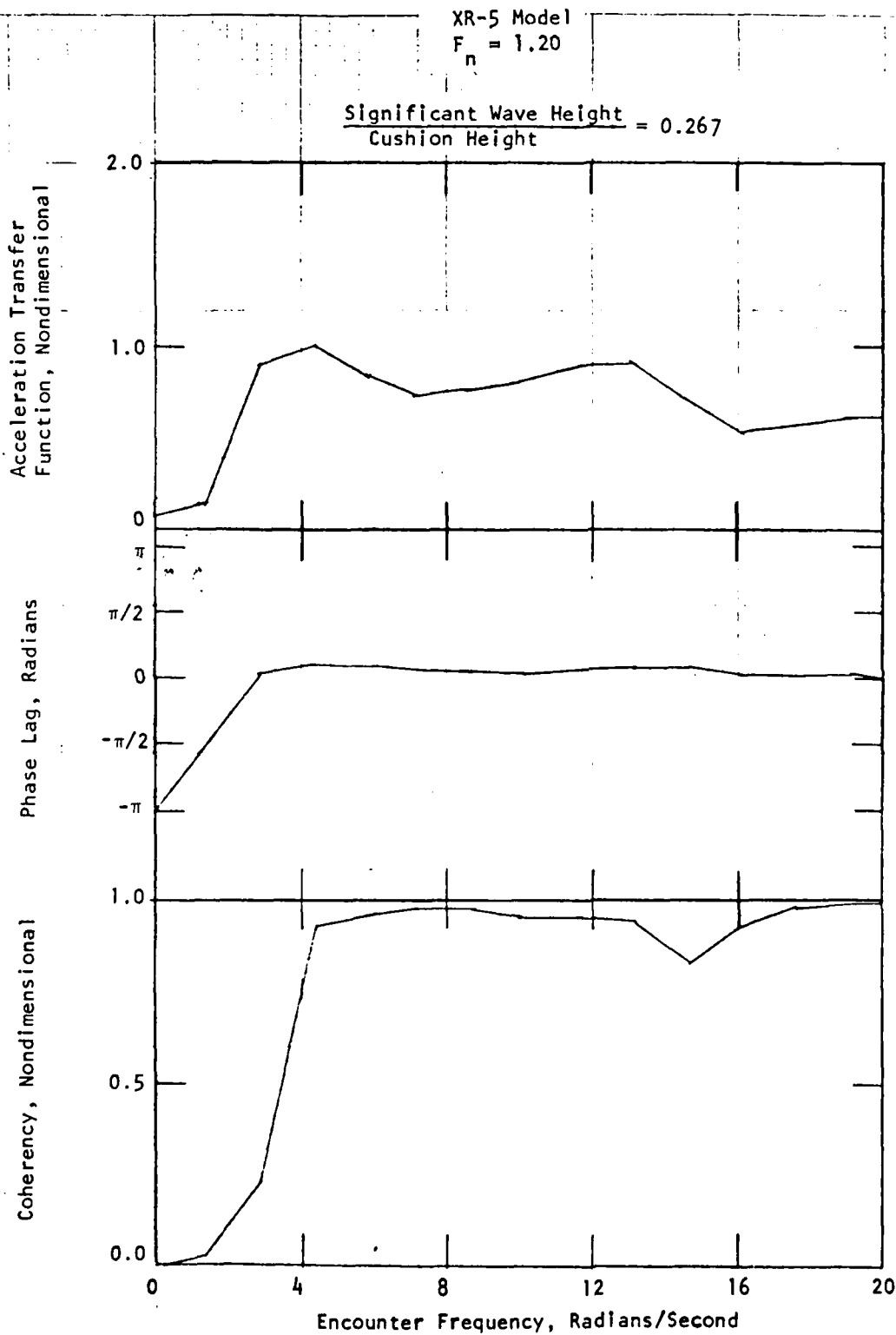


Figure 15 - Heave Acceleration Response, $F_n = 1.20$, Significant Wave Height/Cushion Height = 0.267

XR-5 Model
 $F_n = 0.72$

$\frac{\text{Significant Wave Height}}{\text{Cushion Height}} = 0.392$

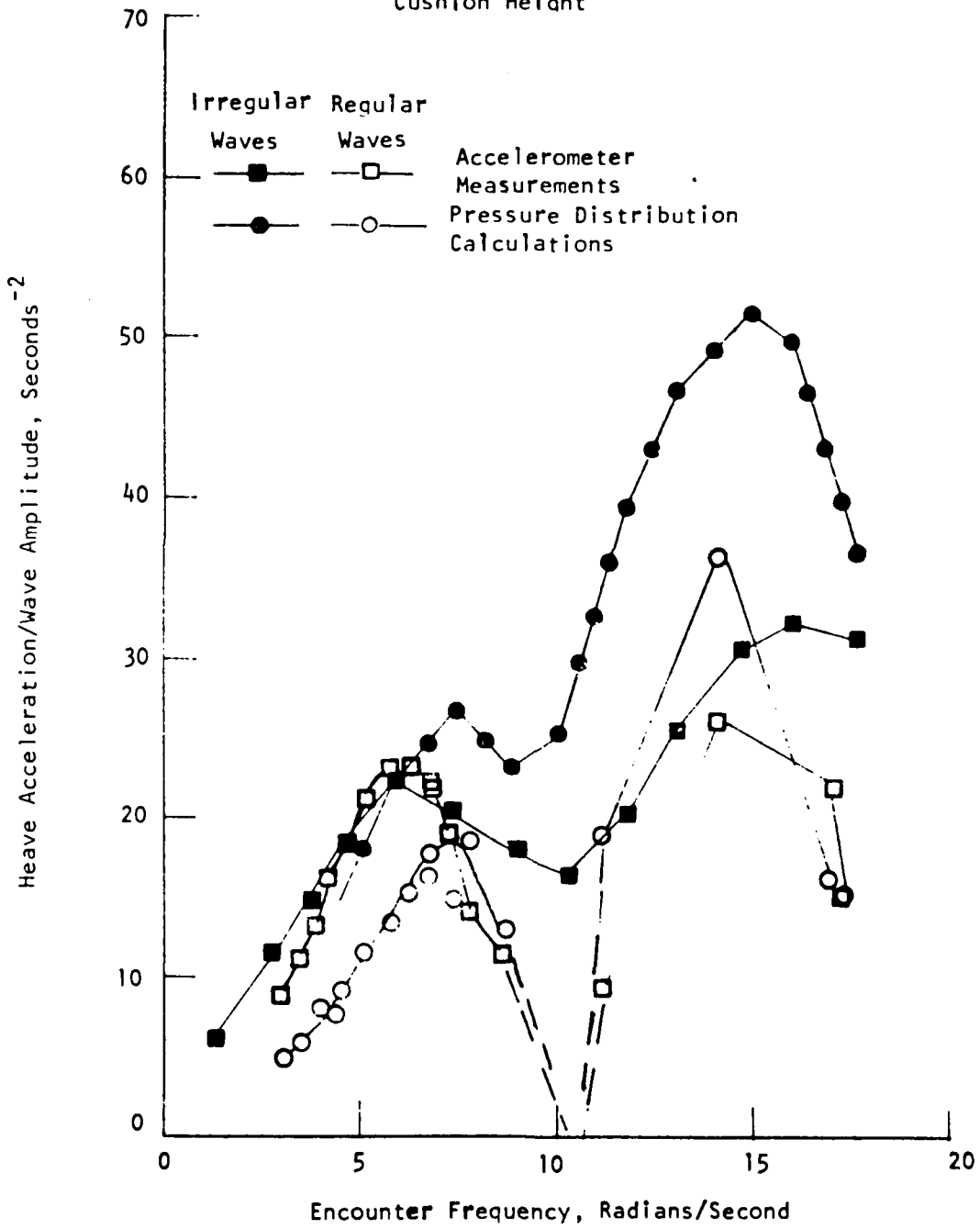


Figure 16 - Heave Acceleration Transfer Functions in Regular and Irregular Waves, $F_n = 0.72$

XR-5 Model
 $F_n = 0.72$

$\frac{\text{Significant Wave Height}}{\text{Cushion Height}} = 0.529$

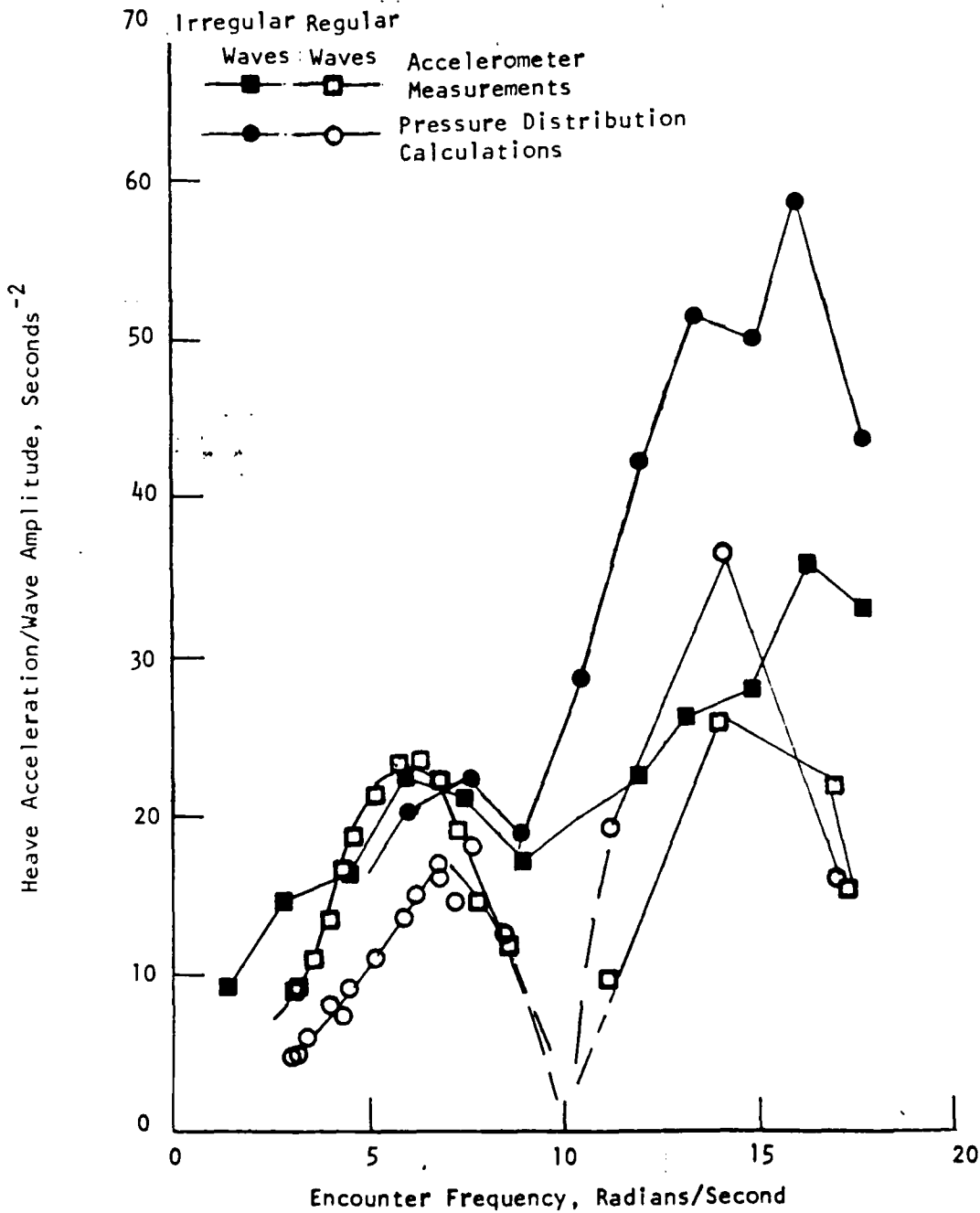


Figure 17 - Heave Acceleration Transfer Functions in Regular and Irregular Waves, $F_n = 0.72$

XR-5 Model
 $F_n = 0.96$

$\frac{\text{Significant Wave Height}}{\text{Cushion Height}} = 0.309$

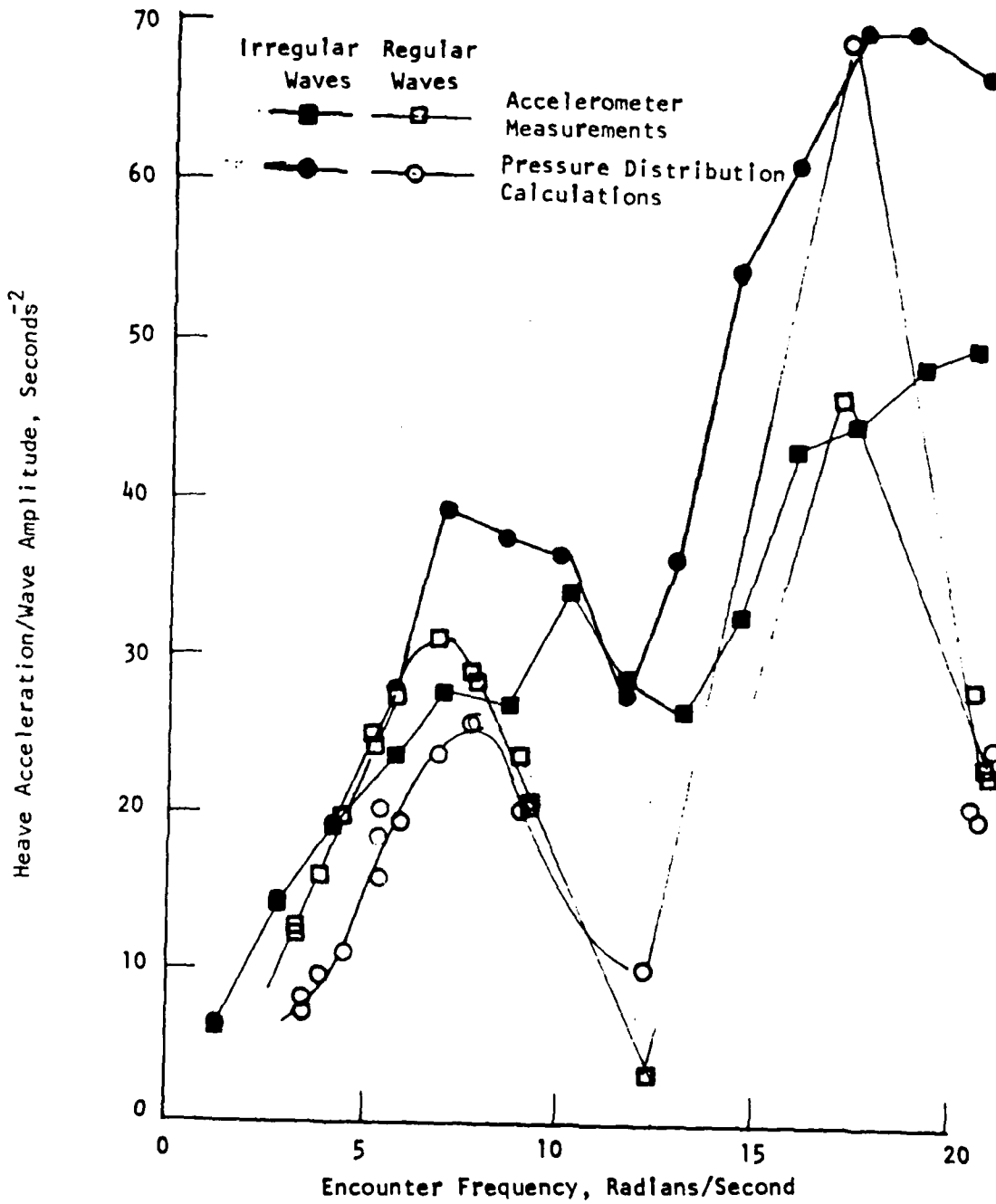


Figure 18 - Heave Acceleration Transfer Functions in Regular and Irregular Waves, $F_n = 0.96$

XR-5 Model
 $F_n = 0.96$

$\frac{\text{Significant Wave Height}}{\text{Cushion Height}} = 0.693$

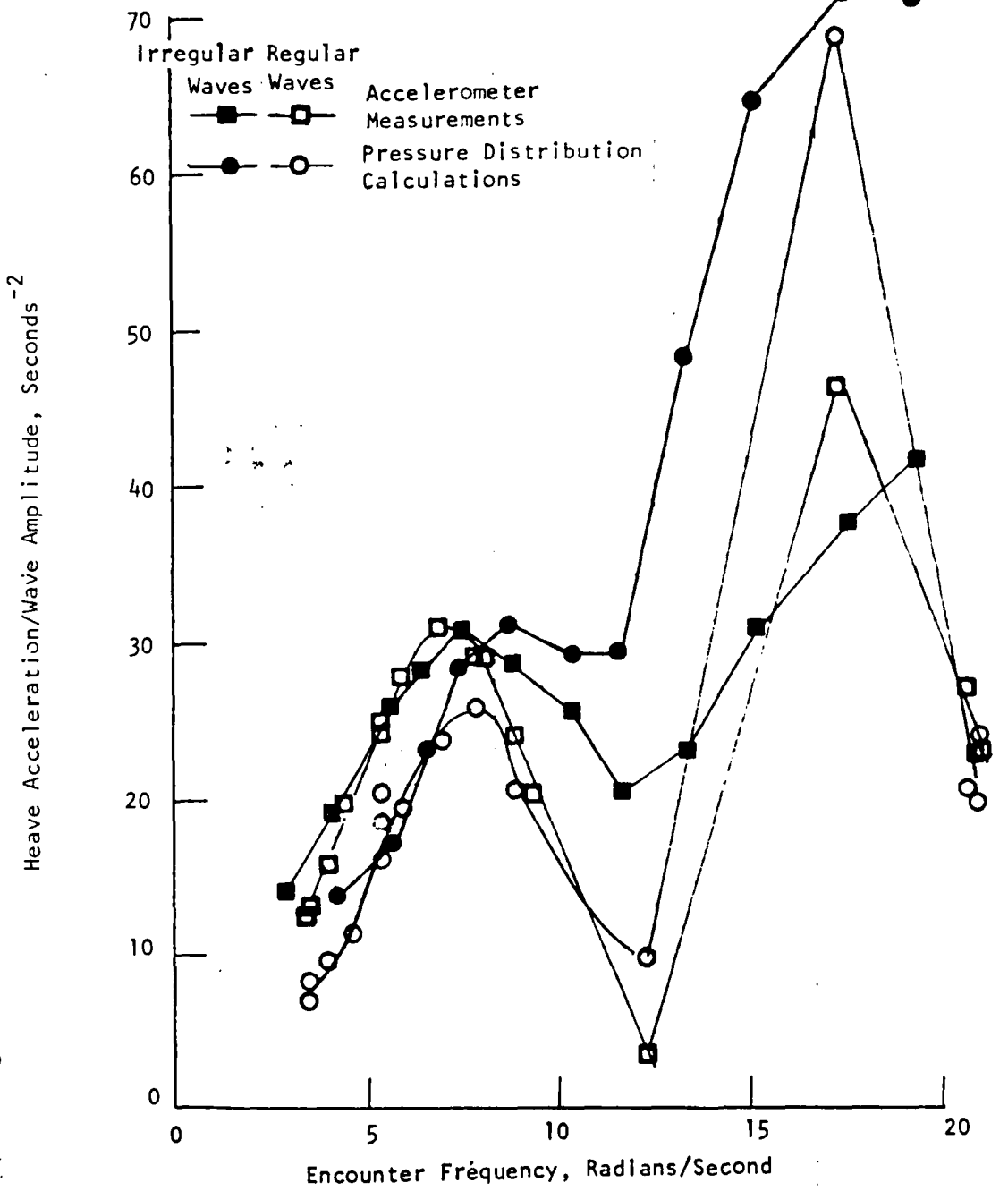


Figure 19 - Heave Acceleration Transfer Functions in Regular and Irregular Waves, $F_n = 0.96$

XR-5 Model
 $F_n = 1.20$

$\frac{\text{Significant Wave Height}}{\text{Cushion Height}} = 0.267$

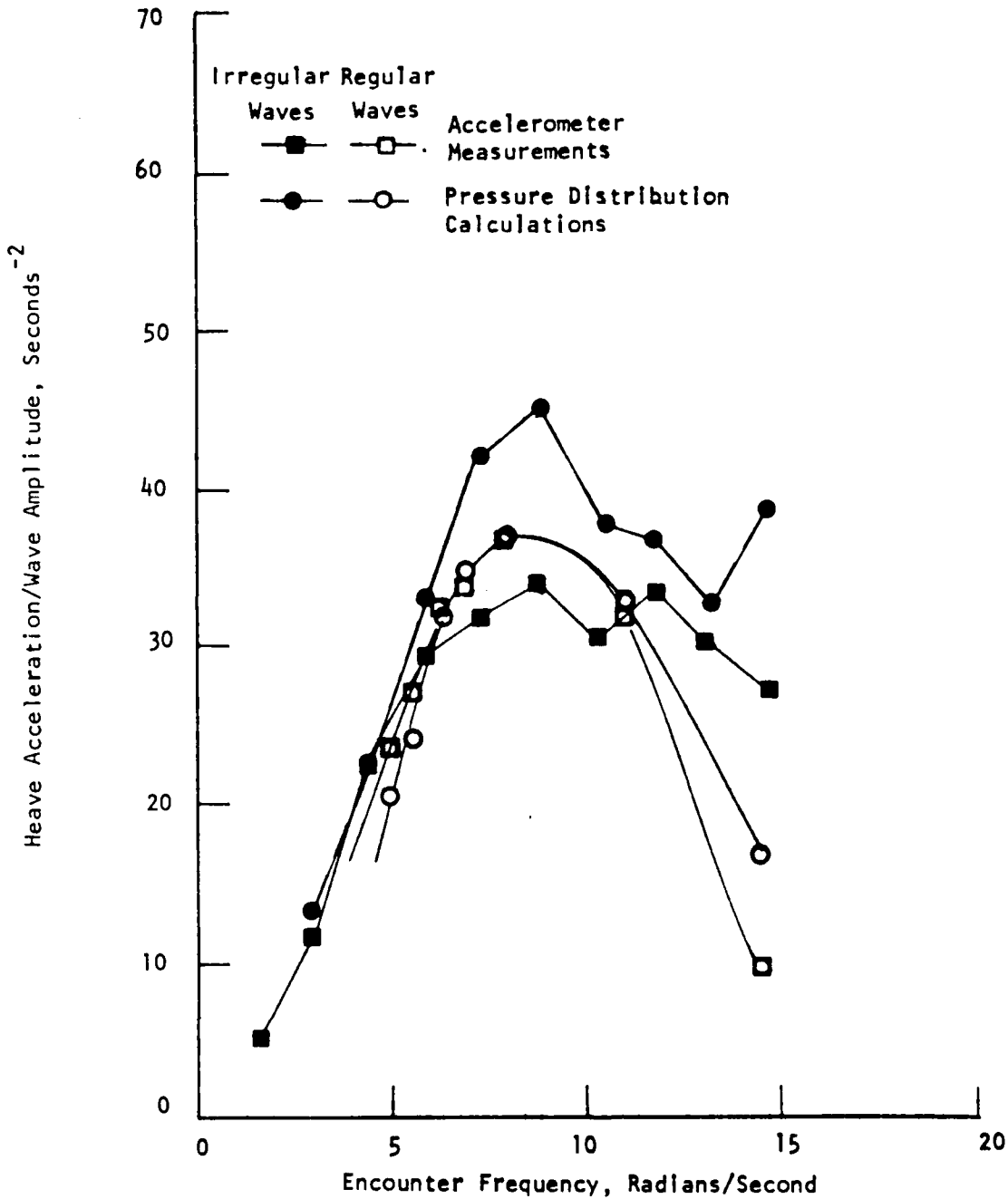


Figure 20 - Heave Acceleration Transfer Functions in Regular and Irregular Waves, $F_n = 1.20$

XR-5 Model
 $F_n = 0.72$

$\frac{\text{Significant Wave Height}}{\text{Cushion Height}} = 0.392$

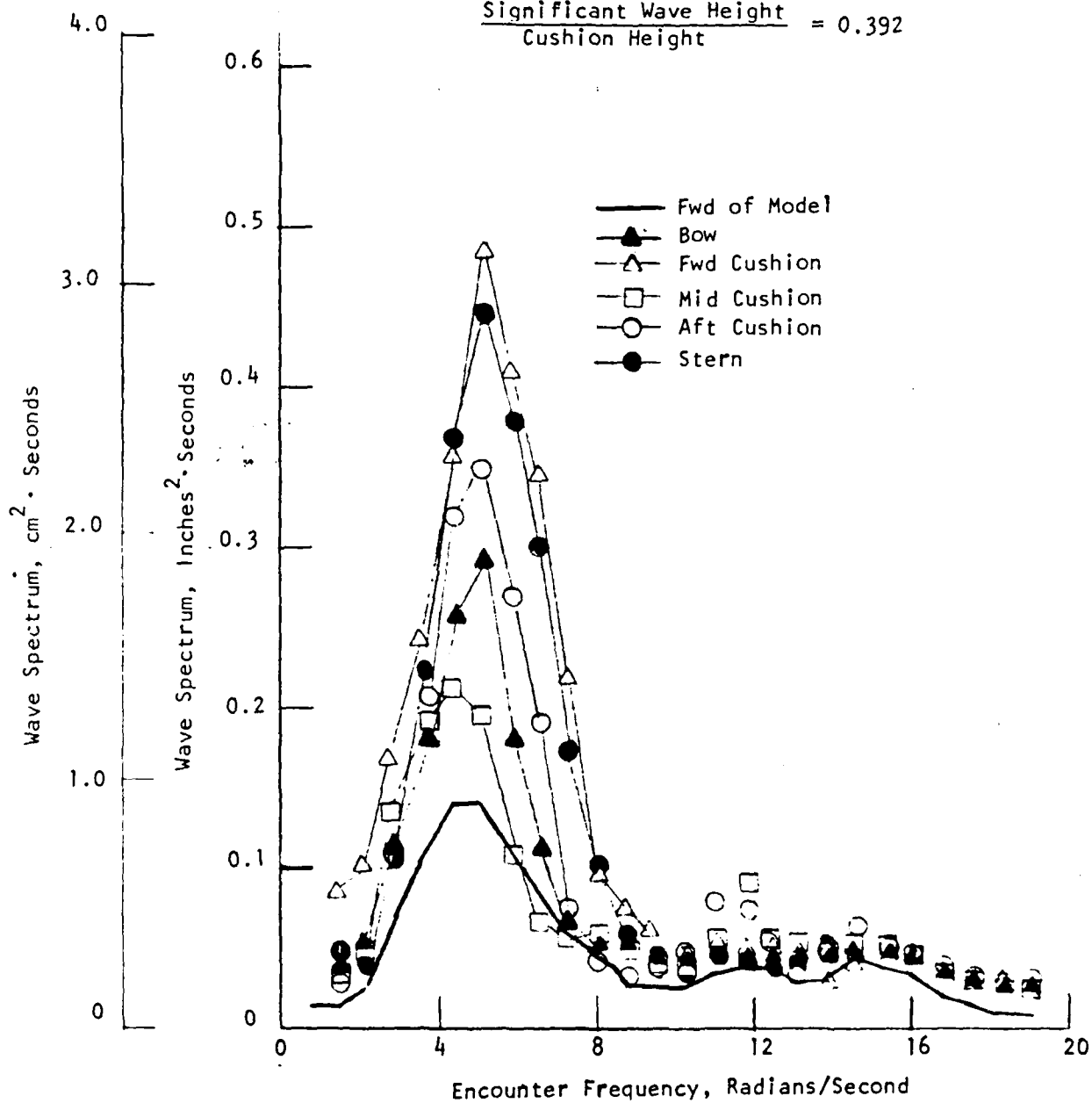


Figure 21 - Wave Spectrum Variation , $F_n = 0.72$, Significant Wave Height/Cushion Height = .392

XR-5 Model

$F_n = 0.72$

$\frac{\text{Significant Wave Height}}{\text{Cushion Height}} = 0.529$

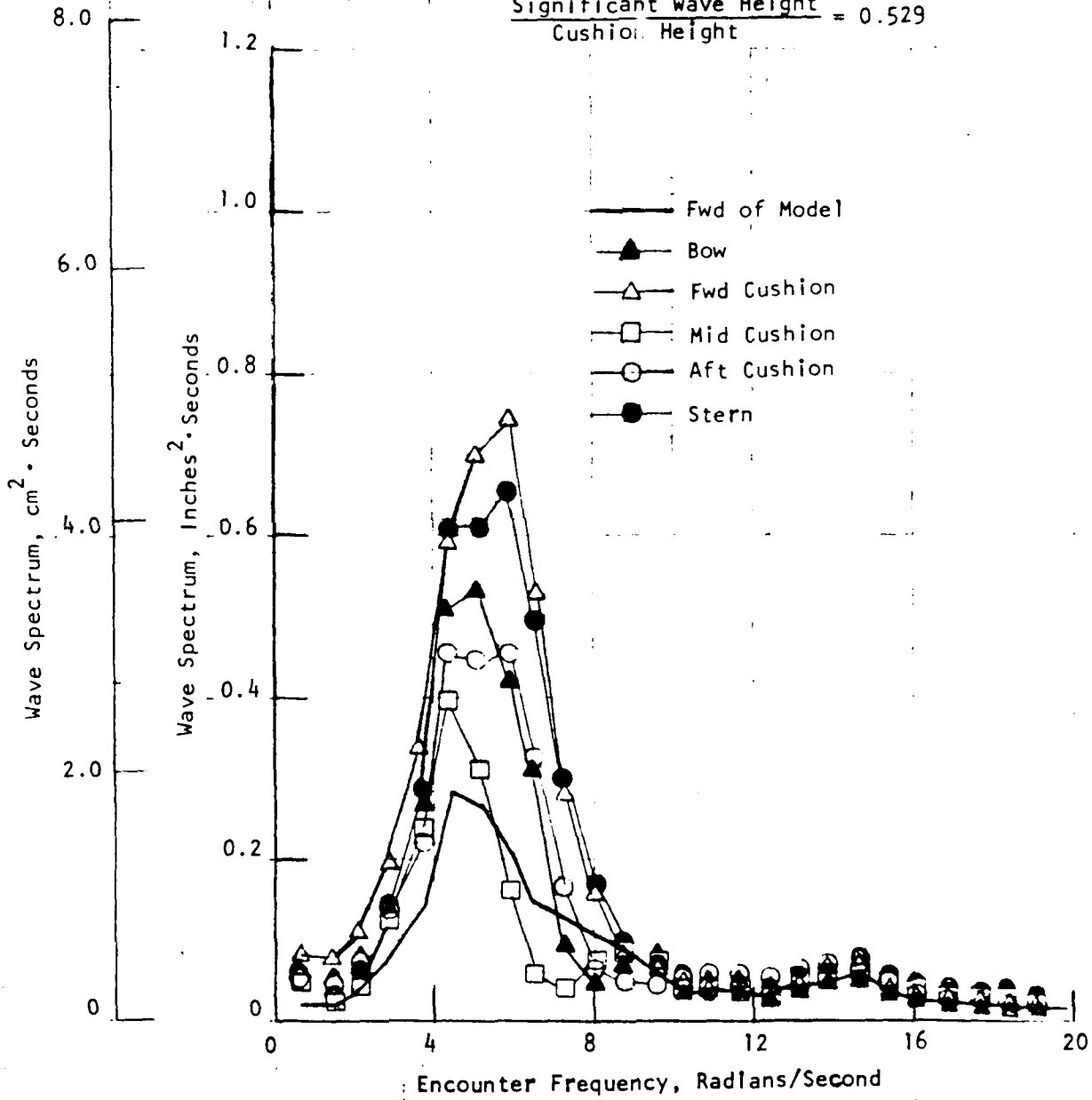


Figure 22 - Wave Spectrum Variation, $F_n = 0.72$, Significant Wave Height/Cushion Height = .529

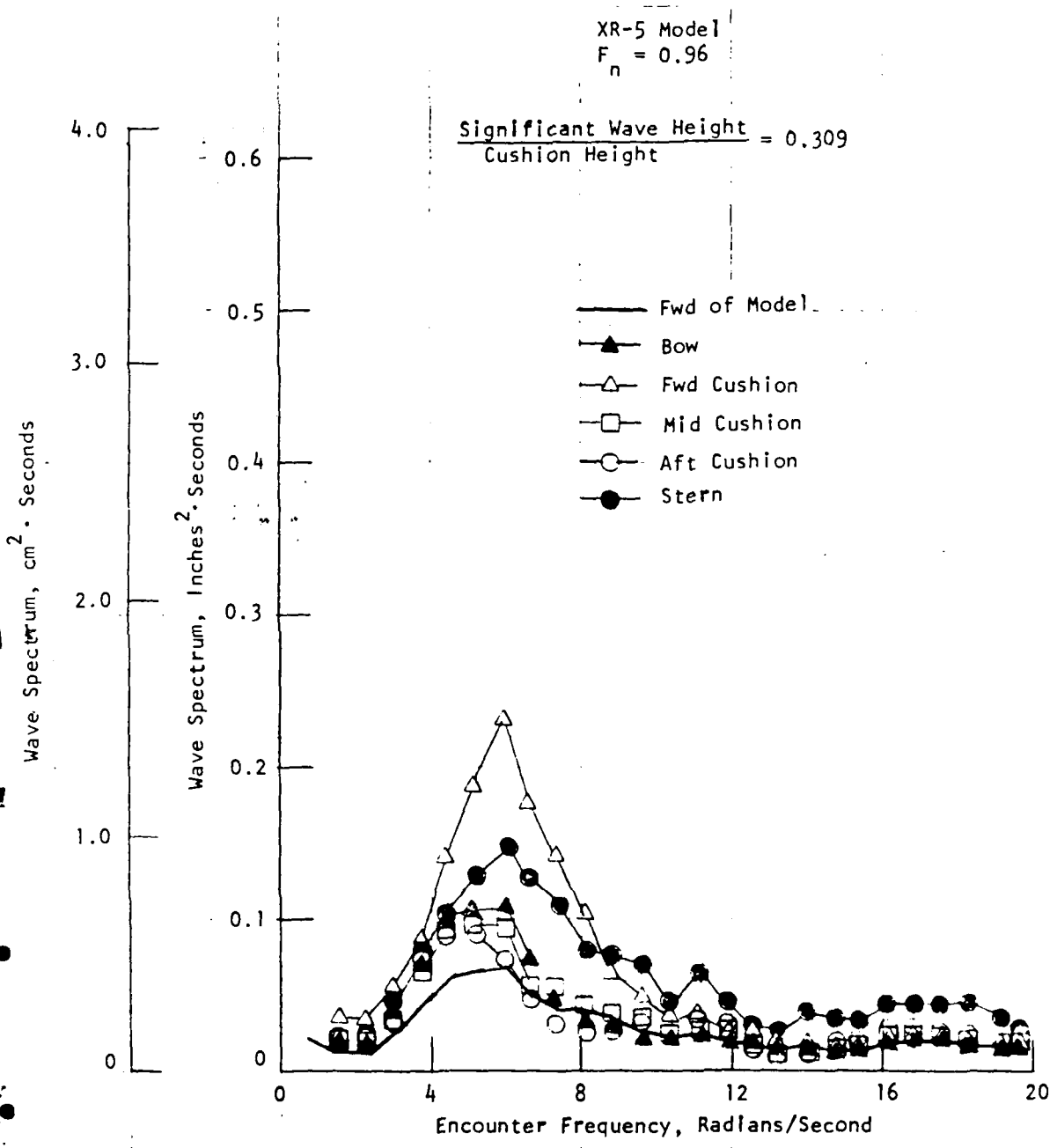


Figure 23 - Wave Spectrum Variation, $F_n = 0.96$, Significant Wave Height/Cushion Heightⁿ = .309

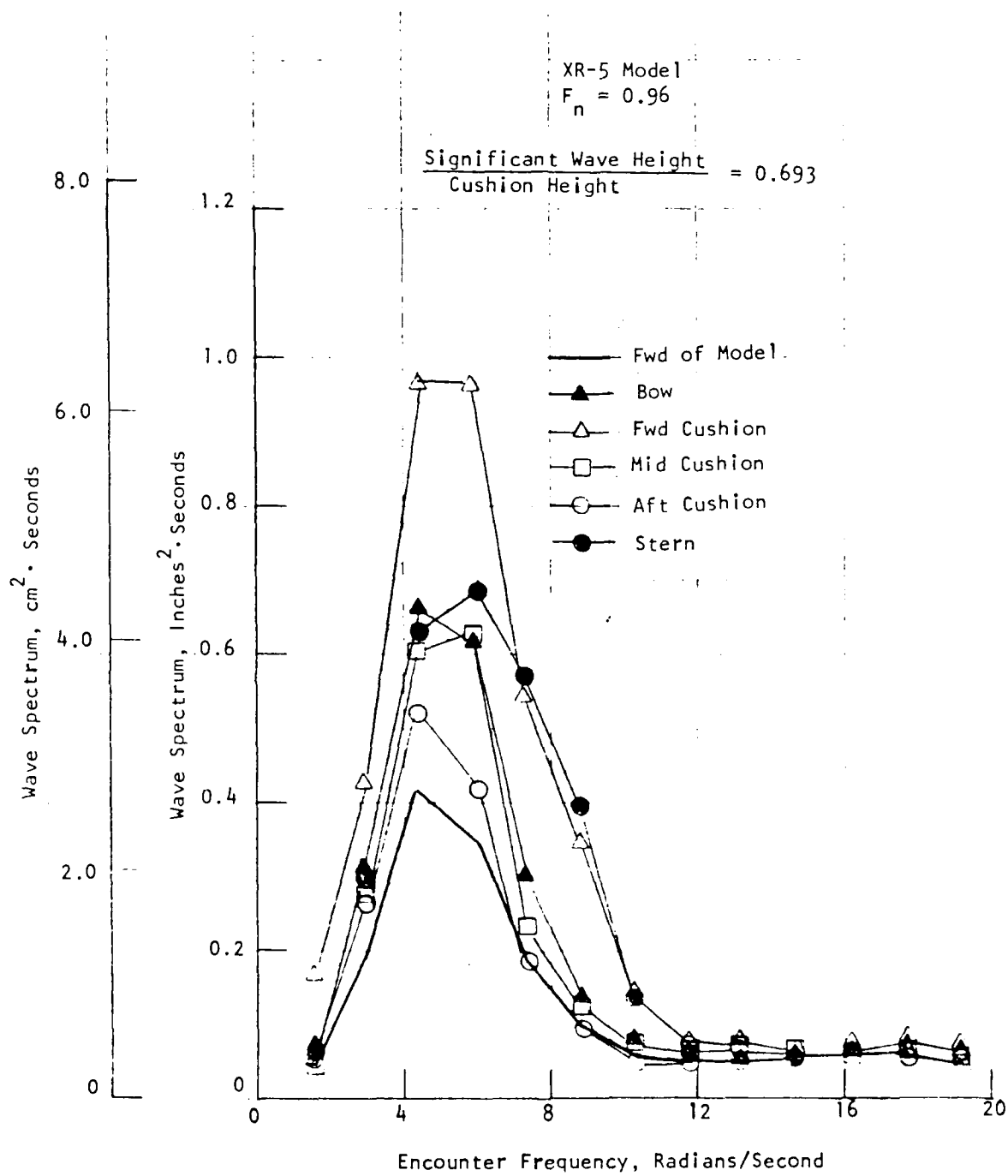


Figure 24 - Wave Spectrum Variation, $F_n = 0.96$, Significant Wave Height/Cushion Heightⁿ = .693

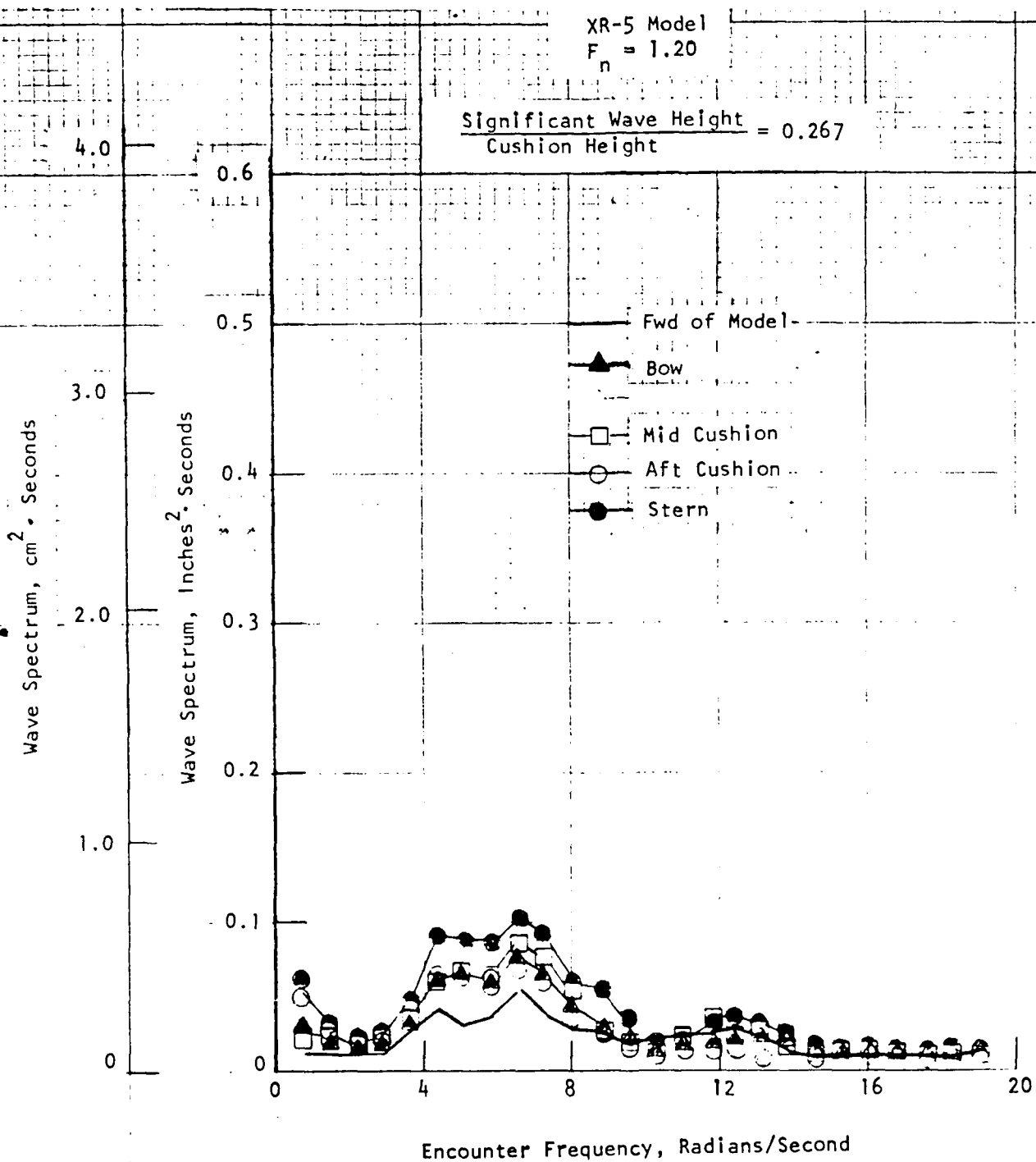


Figure 25 - Wave Spectrum Variation, $F_n = 1.20$, Significant Wave Height/Cushion Heightⁿ = .267

DTNSRDC ISSUES THREE TYPES OF REPORTS

(1) DTNSRDC REPORTS, A FORMAL SERIES PUBLISHING INFORMATION OF PERMANENT TECHNICAL VALUE, DESIGNATED BY A SERIAL REPORT NUMBER.

(2) DEPARTMENTAL REPORTS, A SEMIFORMAL SERIES, RECORDING INFORMATION OF A PRELIMINARY OR TEMPORARY NATURE, OR OF LIMITED INTEREST OR SIGNIFICANCE, CARRYING A DEPARTMENTAL ALPHANUMERIC IDENTIFICATION.

(3) TECHNICAL MEMORANDA, AN INFORMAL SERIES, USUALLY INTERNAL WORKING PAPERS OR DIRECT REPORTS TO SPONSORS, NUMBERED AS TM SERIES REPORTS; NOT FOR GENERAL DISTRIBUTION.

END

FILMED

5-85

DTIC

